SWISS FEDERAL INSTITUTE OF TECHNOLOGIES
SCHOOL OF LIFE SCIENCES

Master project in Life Sciences and Technology

GENE EXPRESSION ANALYSIS OF METASTASES AND IL-1R1 CHARACTERIZATION IN A NALP3 MOUSE MODEL

Done by
Heidi FOURNIER
Terrasses Du Soleil
1997 Haute-Nendaz

Carried out in the laboratory of *Prof. Ivan Stamenkovic* (CHUV-Lausanne)
Under the supervision of *Marie-Aude Le Bitoux*, Postdoc

Under the direction of
Prof. Michel Aguet
ISREC - EPFL

LAUSANNE, CHUV-EPFL 2011

Table of Contents

ACKNOWLEDGEMENTS

This Master Project was made in the laboratory of Prof. Ivan Stamenkovic (Experimental Pathology Unit, CHUV). During the 9 months of the project, I was supervised by Marie-Aude Le-Bitoux and I want to particularly thank her for the time she spent with me and for all I could learn from her. I am now rich of her teaching and experience. A special thank also for the rest of the Lab and for Ivan, because they also spent time with me explaining different techniques and giving me advices, I really appreciated!

1. ABSTRACT

Tumor microenvironment contributes strongly to tumor evolution toward metastasis, a final stage in cancer progression. It provides essential clues to promote migration of cancer cells in metastatic sites. Moreover, inflammatory cells and immunomodulatory mediators present in the microenvironment are able to polarize the host immune response, thereby potentiating primary tumor development. The reciprocal and dynamic interactions between microenvironment and tumor cells orchestrate critical steps of evolution toward metastasis.

To address the role of inflammation in tumor progression, a mouse model of downregulated inflammation was used: the NALP3 gene in these mice is knocked-out, causing an impaired processing of the two inflammatory cytokines Interleukin-1β and IL-18 which are essential for the recruitment and activation of immune cells. In this case, a decrease in tumor growth and metastasis was observed in previous studies, leading us to investigate the molecular and cellular interactions of tumor and immune cells in inflammatory and non-inflammatory contexts.

Gene expression analysis was performed on two types of mouse tumor cells: the B16-F10 melanoma cells seem to be more dependent on the immune cells recruitment to metastasize *in vivo*, while the Lewis Lung Carcinomas cells showed a quite equivalent growth in both wild-type or NALP3 knock-out mice. Different techniques were used to do so, such as standard *in vitro* assays and mRNA expression analyses, and *in vivo* tests with extraction of tumoral mRNA by Laser Capture Microdissection. Gene expression analyses of tumor cells were performed to address the influence of the inflammatory background. Comparison of these two gene expression profiles may reveal genes related to the specific reactive inflammatory response surrounding the given metastases.

Another point that was investigated was the importance of the IL-1R1, receptor of interleukin-1. Since it represents the counterpart of IL-1β signaling, its expression by immune and tumor cells may correlate with degree of tumor growth and invasion. *In vitro* and *in vivo* assays allowed better understanding the importance of this receptor. While a downregulation of this receptor impairs proliferation of in vitro cell cultures, at the *in vivo* level, the number of metastases is decreased too.

These results provide potential clues indicating the important role played by the inflammatory cells, and how they can support and promote tumor progression, in particular through the expression of NALP3. The adaptation mechanisms of tumor cells to their microenvironment were also assessed, opening different insights for targeting the tumor itself as well as the inflammatory microenvironment.

2. INTRODUCTION

With 7.6 million deaths in 2008, cancer is a leading cause of death worldwide, with a vast majority of cancer-related deaths caused by dissemination of tumor cells, phenomena called metastasis [1]. Furthermore, the projections show a continued rise to over 11 million in 2030. Being a major public health problem, it has never been more important to find new solutions in order to eradicate this complex and wide propagated disease. The crucial issue is thus to discover and develop, through the better understanding of the biology of tumors and metastases, effective and novel therapies to treat patients.

The main difficulty resides in the huge complexity of the disease, enclosing such a lot of different types of cancer and multiple genetic variations between all of them. However, the many different steps of transformation could also be seen as many potential and specific therapeutic targets. Moreover, the complex interactions between tumor cells and their microenvironment represent a key issue to determine the potentiality of a tumor to evolve or not toward metastasis. In the past decades, the research was more based on the concept of cancer-cell- and genome-centered models, with publications mainly focused on describing oncogenes and suppressor genes, their mutations and changes of expression in tumor cells. However, even if these concepts are fundamental to understand how the tumor cells acquire self-sufficiency for growth and proliferation, the surrounding tissue is the other key player that allows these cells to remain and proliferate, in a given tissue [2]. At some point, the microenvironment is likely to be the major component allowing and promoting tumorigenesis, thus even more so during angiogenesis and metastasis. That is why, more recently, the scientific community began to study new models including the important component that the microenvironment represents. Since then, we could understand that, besides the genetic modifications encountered in the tumor cells, the stroma is also subject to genetic and phenotypic changes during cancer progression. There are even more and more evidences that support the concept in which tumor microenvironment is driven to undergo specific modifications in contact with the tumor, getting enslaved, and that in the end, the control of tumor cells is so important that its microenvironment reaches a stage of promoting tumor progression [3].

In particular, infiltrating immune cells play decisive roles, and thus at every stages of tumor growth and evolution, through the manipulation of other immune cells, modifying immune surveillance. Inflammatory cells and their mediators contribute to local invasion but also to general dissemination. The many bidirectional and dynamic interaction between tumor - and immune cells also orchestrate the built in of metastatic niches, allowing facilitated propagation [4].

Tumor-Host Interactions: the basics

The Tumor Side

A tumor is defined as an abnormal proliferation of cells in a tissue, also called a neoplasm. This is caused by genetic mutations that are due to many different environmental factors like radiations, pollution or infections. The term of carcinogenesis is used to describe the multistep process by which normal cells are transformed into cancer cells, through acquisition of new characteristics.

Key modifications due to accumulation of mutations (Fig. 1-A) consist of resistance to apoptosis, insensitivity to growth signals and self-sufficiency in growth signals. Subsequently, changes at cellular and genetic level reprogram the cell so that cellular division gets uncontrolled. Therefore a malignant mass appears, called dysplasia (Fig. 1-B). The alteration in tissue homeostasis is responsible to elicit an inflammatory response, further promoting tumor growth through activation of surrounding stroma. Then, with additional characteristics and acquisition of more motile and migratory phenotype, new blood vessels can be formed to better feed the tumor cells, a process called angiogenesis. Finally, during metastasis, the cells invade tissue and forms colonies at distant sites (Fig. 1-C) [5].

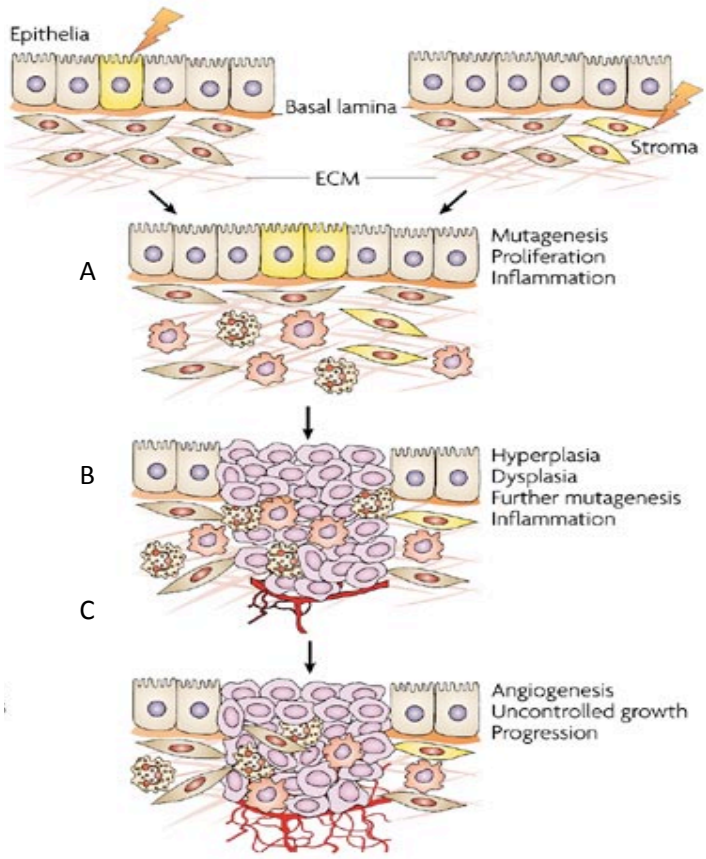

Figure 1 : The process of carcinogenesis [5]

The homeostatic equilibrium found in normal tissues is disrupted by tumorigenesis. Under normal conditions, mesenchymal-epithelial interactions are tightly controlled so that tissue integrity is maintained with normal cell proliferation and turn over. Moreover, the basement membrane acts as a barrier between supportive tissue and epithelial cells. The fibroblasts, inflammatory and endothelial cells that compose normally the stroma are present in a quiescent state.

All these features of normal epithelia are disrupted by carcinogenesis: the increase in proliferation of tumor cells leads to activation of fibroblasts and a transition called epithelial to mesenchymal transition (EMT) takes place for some cells, increasing their motility and invasiveness, with degradation of basement membrane. These events lead to a complete disorganization of the tissue with loss of separation between compartments. New contacts get established between cells with direct and dynamic interactions. This new crosstalk allows the tumor cells to turn the situation to their advantages, enslaving immune cells to induce an even more suitable microenvironment [6].

The Microenvironment Side

The tumor microenvironment comprises many different cells beside cancerous cells. It is composed of lymphatic and vascular endothelial cells, fibroblast and both innate and adaptive infiltrating immune cells. Extracellular matrix (ECM) and basement membrane also belong to the complex organization of tumor-host microenvironment, including proteoglycans, glycoproteins and collagens (Fig. 3).

Under normal conditions, these different types of cells maintain tissue homeostasis in the different organs of the body. In case of injury, could it be caused by an infection or an intrinsic danger signal, a multifactorial network of chemical signals induces a response in order to heal the afflicted tissue. Mast cells, resident cells, get activated and thus send signals that attract macrophages and immune cells at the site of infection [8]. The extracellular matrix serves as a scaffold on which fibroblasts and endothelial cells can proliferate and migrate, thus forming the basis for reconstruction. Mesenchymal cells such as fibroblasts are also recruited and driven to form collagen. New blood vessels are also built and the whole finally remodels the tissue to "heal the wound".

While under normal situations these events happen normally, tending toward homeostasis of tissue environment, carcinogenesis appears like a chaotic disorganization of the process of inflammation and repair. That is why tumors are of called "*Wounds that never heal*", in the words of Hal Dovrak. In contrast with the organized series of events explained in the previous paragraph, during carcinogenesis, this disorganization prevents re-establishment of homeostasis [9].

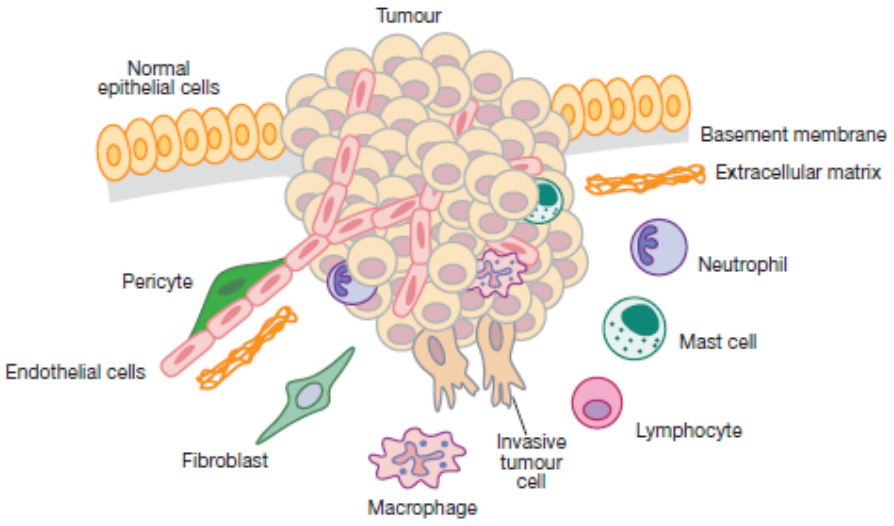

Figure 2: The tumor microenvironment [7]

At the beginning, both stroma and epithelium undergo modifications promoting proliferation and amplifying mutagenesis [8]. Fibroblasts are activated and secrete more collagen, rendering the stromal reaction desmoplastic. At this stage, the extracellular matrix changes in composition, with more ECM proteins such as fibronectins, collagen of type I and proteoglycans, beside higher number of infiltrating immune cells.

Tumor – Microenvironment Interactions: Cancer related inflammation

Since the main point of the present study is related to inflammation, a more detailed section is devoted in describing the different aspects that make the both, tumor and inflammation, so tightly linked.

While most immune mediators and inflammatory cells would be able to reject and eliminate cancer cells, actually the immune system gets enslaved and it even promotes tumor evolution: initiation, promotion toward malignant conversion, migration and metastasis. That is why tumor microenvironment is the other key player becoming as important as transformed cells; its control and a deeper understanding of the different interactions will certainly help to create novel and different therapeutic approaches [10].

Globally, two pathways connect cancer and inflammation. First, the intrinsic pathway is the activation as a result of genetic modifications that cause neoplasia, such as oncogene activation. Transformation of cells in this way produces, as explained in the last section, inflammatory mediators and generates an inflammatory microenvironment. The other pathway is called extrinsic because the cause leading to tumor development is extrinsic and due originally to viral infection. At some point, both pathways converge, since the same state is reached in both cases. Different transcription factors are activated, as for instance NF-κB or STAT3. Different oncogenes are also activated in tumor cells such as MYC or RAS, responsible for the stimulation of transcriptional programs that recruit immune cells. Mediators are produced by tumor cells that attract immune cells and these are then modified and utilized by cancer cells so that the basic same transcription factors are also activated, resulting in an auto-amplifying loop that benefits tumor progression and cancer-related inflammation [11]. However, relationships between tumor and immune cells are dynamic. With time, the selective pressure from immune system induces tumor cells to undergo a process that is called immune editing. This term describes the fact that tumor cell become resistant to first-line of defense of immunity by the evolution of phenotypes that are able to manipulate the immune cells.

Inflammation and neoplastic progression

The leukocyte population of a developing neoplasm includes dendritic cells, macrophages, neutrophils, eosinophils, mast cell and lymphocytes. Both innate and adaptive immune system is represented and each cell type produce an assortment of different mediators, cytokines, reactive oxygen species, serine and cysteine proteases, MMPs and mediators of cell killing such as TNF-α and interleukins. Here following is described in details the creation of a local inflammatory microenvironment, results of reciprocal and dynamic interactions [15].

Initially, cancerous cells, in response to hypoxia and necrosis secondary to excessive cell proliferation, secrete different chemokines and cytokines that attract monocytes and macrophages. The latter also secrete growth factors, such as VEGF-A or FGF, to affect tumor cells behavior, but also activate tumor endothelium and prolong inflammation. COX-2, a potent stimulator of cell proliferation, survival and motility is also released by macrophages in the microenvironment.

In presence of granulocyte-macrophage colony-stimulating factor (GM-SF) and interleukin IL-4, monocytes differentiate into immature dendritic cells that migrate into inflamed peripheral tissue to capture antigens. It will then be presented in lymph nodes to T-lymphocytes. An interesting point

is that most dendritic cells present in neoplasms are defective in T-cell stimulatory capacity. Moreover, in most cases, adaptive immune response is too weak and inefficient to really eradicate tumor cells [15].

Another important component of neoplastic infiltrate is the tumor-associated macrophages (TAM). Derived from monocytes, TAMs have a paradoxical role in carcinogenesis. Although IL-2 and IL-12 activate macrophages to kill tumor cells, these cells also produces different potent angiogenic and lymphangiogenic factors as cytokines, growth factors and proteases, which are able to promote tumor progression. Macrophages are also responsible for the production of IL-10, a mediator molecule that is known to dissipate anti-tumor activities of T cells [13]. Macrophage-cancerous cells crosstalk promotes the release of macrophage-derived cytokines, chemokines and growth-motility factors. This works in an auto-amplifying loop since these mediators recruit more inflammatory cells.

The coordination of stromal response to cancer is, among other, realized by chemokines and cytokines present in the microenvironment. Both polarize the immune response, but it also strongly influences the composition of cellular infiltrate and is described to induce angiogenesis. Moreover, their corresponding receptors are often upregulated in cancer cells [15].

The stroma gets rapidly infiltrated with different leukocytes populations and this can be viewed as a double-edged sword: either it can produce cytokines that work to inhibit tumor growth (IL-12 that is anti-angiogenic) or fully dedicated to tumor progression. *The abundance and state of activation of the different cells and the level of expression of different immune mediators and modulators balance the direction of pro or anti-tumor immunity that emerges there.*

In addition, as inflammation is sustained, non-specific pro-inflammatory cytokines as IL1α-β, IL-6 or interferon (IFN)-γ get up-regulated, leading to increased transformation of normal cells toward pre-neoplastic foci. The transcription factor NF-κB, main link between tumorigenesis and inflammation, is an important element allowing cells to escape apoptosis [14].

Many tumors are described as associated with the activation of tumor-promoting innate immune response with neutrophils and macrophages, while on the other hand, specific adaptive immune response with T and B lymphocytes are simply not efficient in the eradication of tumor niches.

There are different strategies used by the tumor cells to escape efficiently the immune surveillance. Down-regulation and even loss of tumor-associated antigens (TAA) is often described, as well as the use of immunosuppressive cytokines, such as IL-6 and TGF-β. These mediators interfere at multiple steps and pathways in the elaboration of immune response [12]. TGF-β is particularly efficient in immunosuppression by affecting activation and differentiation of immune cells. Beside its role on immune system, it also affects tumor cells by increasing invasiveness and stroma by inducing EMT.

Focusing on inflammation: the NALP3 Inflammasome

Our innate immune system has evolved germline-encoded pattern recognition receptors (PRRs) that are responsible for the recognition of pathogen-associated molecular patterns (PAMPs): for instance, Toll-Like Receptor-4 (TLR-4) recognizes LPS, a PAMP found on gram-negative bacteria. But some of these receptors are interestingly also able to recognize and sense endogenous signals; these are like intracellular counterparts of TLRs, being intracellular immune receptor sensing danger signals. These two types of receptors cooperate to initiate an immune response. Intracellular alarms

are the result of cell or tissue damages and are called danger-associated molecular patterns (DAMPs). One major family of PRR is the nucleotide-binding domain leucin-rich repeats, NLRs. These cytosolic proteins sense intracellular microbial or *cellular danger signals* and converge, using different signaling pathways, in the transcription of cytokines and chemokines, to further engender proper immune response [16]. In such conditions, molecules that would normally not be accessible are released from sequestration and gain full access to these sensors, triggering an intracellular immune response of defense.

These receptors moreover take part in the formation of bulky molecular complexes called inflammasomes. In fact, inflammasome formation and activation is induced by the sensing of tissue damages (DAMPS) or pathogens (PAMPS). These multiprotein complexes are deeply involved in immune response since they process cytokines such as interleukins. The release of Interleukin-1β is dependent upon the inflammasome NALP3 correct formation and activation.

That is why we particularly focused on this given inflammasome, since we are also interested in dissecting the role of interleukin-1 Receptor 1, IL-1R1, as described in the following sections.

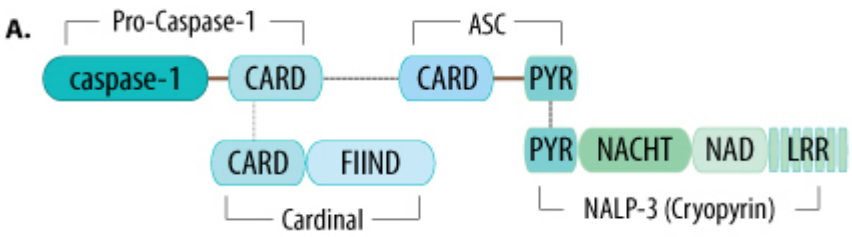

Figure 3 : Structure of NALP3 inflammasome[1]

Having the same basic structure as other NLRs, the NALP3 protein consists of a multidomain assembly with a LRR region as a C-terminal, a central nucleotide domain, a NACHT-associated NAD domain, the NACHT domain and a N-terminal being a PYRIN domain.

Each part fulfills precise tasks. The LRR is responsible for the ligand sensing of DAMPS and PAMPS while NACHT allows the oligomerization that results in active inflammasome. NACHT contains a nucleotide binding domain and thus binds ATP and dATP, sign of cell death when released. PYR facilitate dimerization with corresponding PYR domains in other proteins by homotypic interactions.

The adaptor protein ASC is recruited upon activation of NALP3 protein. This molecule contains, beside the interacting PYR domain, a C-terminal CARD part that is required for inflammasome formation. It is necessary for the interactions with other proteins the complex involves. Thus, ASC recruits, via the CARD domain, the effector protein that is the Caspase-1, also carrying the required CARD domain that interacts. The formation of the inflammasome through these different interactions promotes oligomerization of Caspase-1, leading to the induction of an active enzyme [19].

[1] http://www.rndsystems.com/cb_detail_objectname_cb08i1_Caspase1.aspx

[2] RNaqueous Micro Kit GUIDE: http://www.ambion.com/techlib/prot/fm_1931.pdf

Caspase-1 is responsible for the cleavage of the cytosolic proforms of IL-1β and IL-18. Pro-IL-1β precursor is a 33kD protein while the mature one is 17kD. Active Il-1β results from the cleavage at the specific Tyr-Val-His-Asp site.

Concerning the specific stimuli activating NALP3 inflammasome, the assembly occurs upon sensing of pathogen-associated molecular patterns (PAMPS), nonmicrobial danger or damage signals (DAMPS) as monosodium urate crystals, low potassium or released ATP, reactive oxygen species (ROS) or molecules resulting from lysosomal disintegration, skin irritants and ultraviolet irritation, among others [17, 20].

Basically, a stimulation of PRR (IL-1R1 or TLR4 for instance) induce upregulation of NALP3 and IL-1β expression; this is the priming step (Fig. 4). But the real activation of the inflammasome itself requires another signal of induction. It was demonstrated that inflammasome is not constitutively active in macrophages: the activation of NALP3 in such cells requires both stimulation of the synthesis of the proform of IL-1β (via the NF-κB signaling cascade) and a signal consisting of efflux of potassium: a sudden fall in intracellular potassium level that is triggered by extracellular ATP [21]. The pro-Caspase-1 binds only then the complex through its CARD domain, getting thus activated. The secretion of processed and active IL-1β occurs steadily within hours, through specialized secretory lysosomes [17,21].

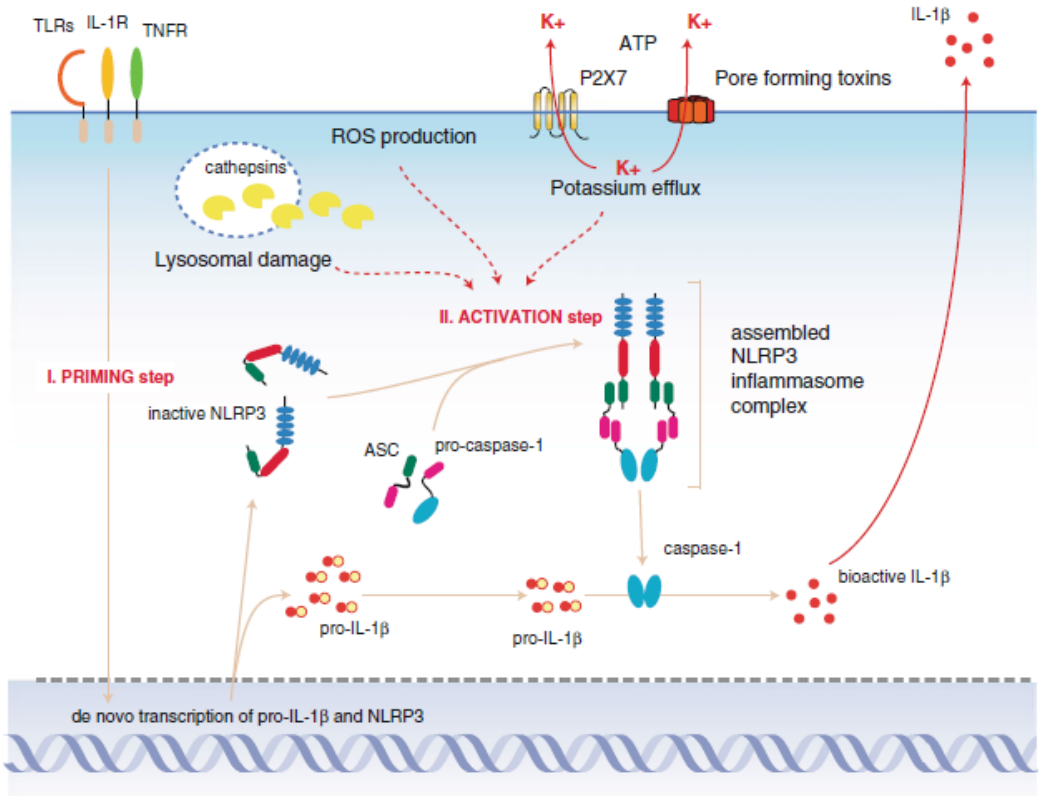

Figure 4: The NALP3 inflammasome and the activation cascade [17]

Tumor-host interactions: Interleukin-1 – A major pleiotropic cytokine

Cytokines have cardinal and dual effects on tumor development: on the one hand, these molecules are involved in malignant transformation and tumor evolution and on the other hand, they participate in the activation of immune effector mechanisms that limit tumor growth. At malignant sites, the network of different cytokines operates and dictates the "net cytokine effect" that fluctuates depending on the stage of tumor development. IL-1 family belongs to this network since its members are major pleiotropic cytokines [22,37].

The IL-1 family is composed of four agonistic proteins (IL-1α-β, IL-18 and IL-33) and one antagonistic protein, IL-1Ra, the IL-1 receptor antagonist.

By binding the receptor without transmitting an activation signal, the IL-1Ra reprensents a physiological inhibitor of IL-1β. Precursors are synthesized as 31kDa proteins, further processed by Caspase-1 for and calpain into mature 17kDa proteins. IL-1β expression and secretion is mainly controlled at the levels of transcription, mRNA stability, processing and secretion. Mononuclear cells are the major productors of such mediators. At low local doses, secretion of Il-1β provokes only local immune response including activation of protective immunity, while higher secretion doses implicate much broader inflammation with tissue-damage and increased tumor-invasiveness [37]. Note that IL-1α secretion level is lower than for IL-1β. IL-18 is also mainly expressed in macrophages. Sharing structural homologies with IL-1β, pro-IL-18 is cleaved after Asp35 by Caspase-1 too, but this cleavage is not exclusive, meaning that other enzymes are implicated [38,39]. The main effector role of IL-18 is the induction of IFN-γ, sharing many intermediate mediators with the IL-1β cascade. Concerning IL-33, its proform is also processed by caspase-1 and the mature form is shown to signal through the IL-1R4 to activate the NF-κB signaling cascade[40].

On the side of the receptors, IL-1Rs are members of the immunoglobulin (Ig) supergene family. This kind of receptors are abundantly and constitutively expressed on many cell types. IL-1R1 is the signaling receptor, while IL-1R2 is a secreted decoy receptor, acting to reduce excessive amount of IL-1 in the microenvironment [22].

The signaling cascade works as follow: upon binding of IL-1β to IL-1R1, a ligand-induced conformational change in the extracellulare domain of the receptor facilitates the recruitement of the IL-1R acceptor protein (IL-1RAcP): an heterodimeric complex forms to transduce the signal. This complex leads to the activation of the IL-1 receptor associated kinase, the IRAK protein, and also recruits the intracellular signaling molecule, MYD88 [22]. These events form a stable IL-1-induced first signaling module. The cascade leads in the end to activation of nuclear genes, mainly through nuclear factor NF-κB cascade: the inhibitor of nuclear factor B (IκB) has to be degraded as a downstream step of the cascade to release p50 and p65 NF-κB. These subunits are then able to translocate into the nucleus to bind conserved DNA motifs. In the presence of IL-1R2 and IL-1Ra, the heterodimeric complex can not form and no downstream activation can occur.

These alarm cytokines are mainly secreted by macrophages to initiate inflammation and induce the expression of pro-inflammatory genes such as COX2 or IL-6. Moreover, IL-1 stimulates its own production, giving rise to an autoamplifiying loop of the imflammatory response, in an autocrine or paracrine manner. In macrophages, an unique IL-1 promoter chromatin structure allows a very rapid cytokine production. The gene-regulatory actions of IL-1 use a conserved signaling system and this relies on rapid and transient assembly of different complexes. Additionally, IL-1 family members

have potentiating effects on proliferation of many different types of cells, such as T and B cells or macrophages[22]. At early stages of carcinogenesis, the role of IL-1 on cell transformation is important since these mediator molecules produce growth factors for the tumor cells. They also generate reactive oxygen intermediate, therefore potentiating mutatgenesis in resident cells at the tumor site. Recent studies have shown correlation between IL-1 expression in tumor cells and oncogene activations so that IL-1 works in an autocrine fashion [24, 23].

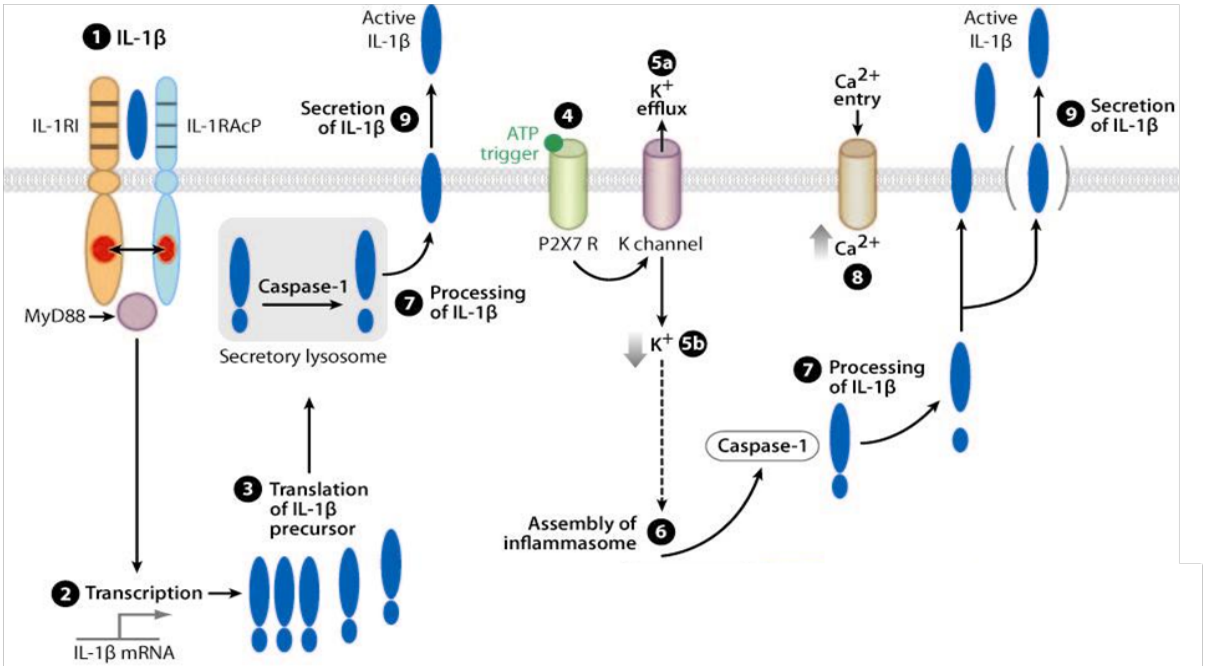

Figure 5: Steps in the synthesis and secretion of IL-1β induced by IL-1β [37]

A mouse model of melanoma hepatic metastasis was used to assess the role of stroma-derived IL-1 in promoting metastasis. Vanaclocha *et al.* could demonstrate the potentiation of liver metastases following intrasplenic injection of recombinant IL-1β or LPS (inducer of IL-1β). On the other hand, the treatment with IL-1Ra could reduce metastases and increase the survival rates. Another model of IL-1β KO mice also showed reduced liver metastasis for B16-F10 melanoma cells. These cells induce the production and secretion by the endothelial cells of IL-1β, TNFα and IL-18, these molecules being particularly efficient in the upregulation of adhesion molecule's expression [25,26].

It was also demonstrated that lymphoreticular organs such as liver, lungs, skin and spleen, being like ports of entry of pathogens, shows high IL-1 expression while internal organs such as brain or kidney have a lower IL-1 expression. It could be deduced that a higher IL-1 expression is due to fact that it deserve a role of defence at these sites, even at the cost of tissue-damage [27,28]. An intersting point is that much less is described concerning the role of IL-1 receptors, especially concerning the expression level on tumor cells, but also on concerned immune cells. Different open questions that still require further investigations.

MicroRNAs: new regulators of immunity

MicroRNAs, miRNAs, are small, noncoding RNAs of about 22 nucleotides in length. These are mediators of RNA interference, representing a novel mechanism controlling expression of proteins at the translational level [30]. Involved in different processes important for development, cell differentiation or cell cycles, their expression is deregulated in cancer. A variety of mechanisms is involved here: epigenetic silencing, insertion-deletion, amplifications or mutations. A striking point is that almost half of know miRNAs are located inside or close to fragile sites or common breakpoint sites that are associated with cancer. Moreover, miRNAs signatures of different malignancies were also described, showing the real influence these molecules have in tumor progression and the importance of understanding the underlying mechanisms [31].

A few words about their biogenesis first. The miRNAs are transcribed by the RNA polymerase II and the primary transcript is of variable length, called the pri-miRNA. The Drosha RNase II recognizes this molecule and cleaves it in the nucleus, resulting in a hairpin precursor form called pre-miRNA (Fig. 6.a). Then, the pre-miRNA is exported by exportin4 and Dicer processes it to form a transient and short 20 nucleotides duplex (Fig. 6.c). RISC is a large protein complex, RNA-induced silencing complex, that incorporates only one strand of the formed duplex. Finally, the mature miRNA loaded on RISC induces translational repression of the target mRNA, with a level of repression depending on the degree of complementarity between the miRNA and its target (Fig. 6.d).

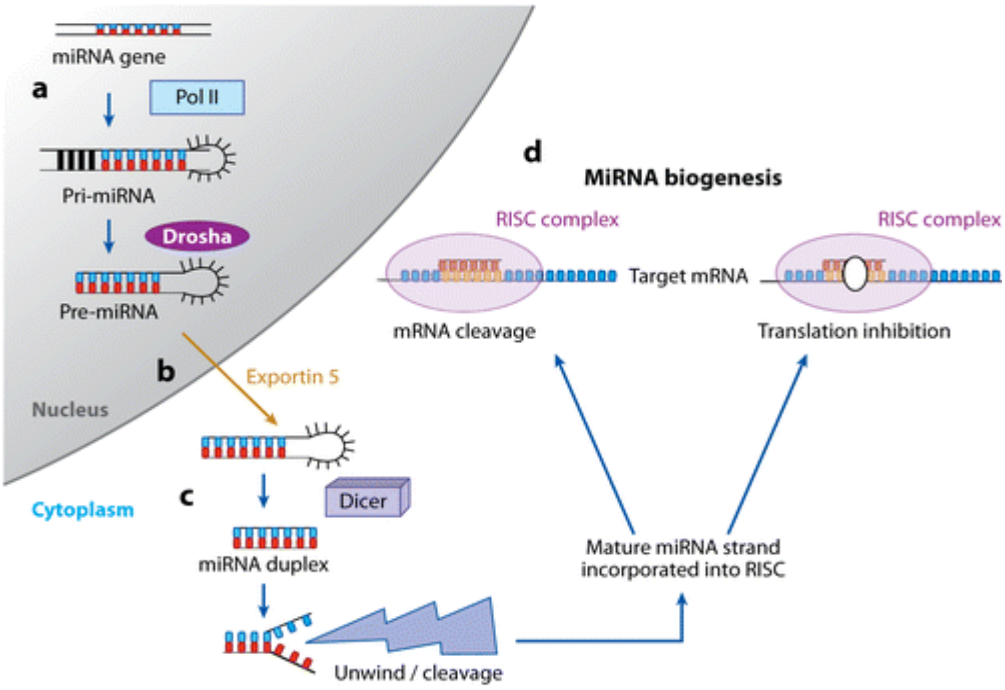

Figure 6: MicroRNAs Biogenesis [31]

Different microRNAs were described for their involvement in immune response's regulation and immune cell maturation [30]. Here we are particularly interested in the miRNAs that regulate the cascade of signaling downstream of the Il-1R1 receptor. MiR-146a was described to be very important in macrophages to regulate the loop of signaling involved in response to IL-1β stimulation. Upon binding of the ligand, as explained in the previous section, the signaling cascade activates the kinase IRAK. This induces the activation of the downstream effector NF-κB, leading to expression of

genes involved in immune response, with inflammatory meditors released. In macrophages, by the same time, miR-146a expression is induced following activation of TLR-2, -4 and -5, upon exposure to TNFα or IL-1β. Interestingly and logically, this is NF-κB that is responsible for its transcriptional regulation (Fig. 7). The expression of miR-146a is then linked to the inhibition of the IRAK- TRAF6- IKK- NF-κB signaling cascade that gets downregulated upon expression of this microRNA [32,33]. miR-146b is induced upon LPS addition in macrophages cultures, and, certainly, other stimulators are still unknown.

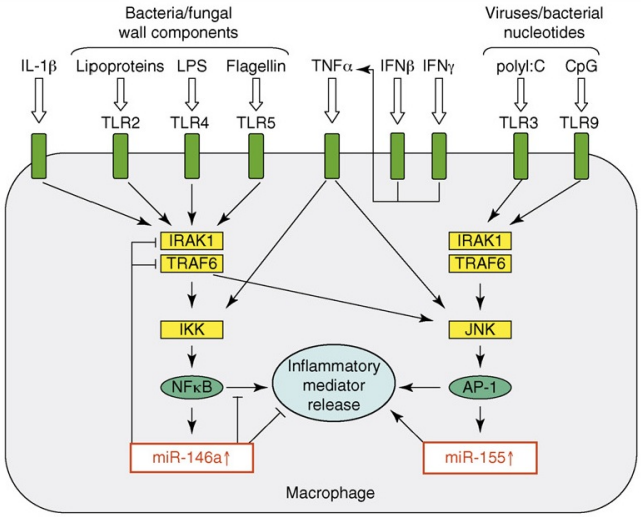

Figure 7: Roles of miR-146a and miR-155 in regulation of inflammatory mediator release [30]

We have the compelling evidences that miRNAs are involved in the regulation of immune response and this opens us new doors: a deeper understanding of their involvment in signaling cascades and modes of action would ultimately give us new tracks to explore and define new therapeutic approaches in the treatment of cancer related inflammation.

AIM OF THE STUDY

Inflammation is a critical player in tumor evolution with inflammatory cells orchestrating the neoplastic process. In particular regarding the inflammasome cascade, several studies could highlight the manipulations that tumor cells operate: the constitutive activation of NALP3 and IL-1 receptor signaling lead to continuous secretion of IL-1β, thus exhibiting features of auto-inflammatory diseases. Moreover, previous studies carried out in the lab highlighted the implication of NALP3 in the processes of tumor growth and metastasis. Indeed, since tumor growth and metastases number are strongly decreased in NALP3-knockdown mice in comparison to wild-type positive control mice, it could imply that NALP3 plays an important role in tumor evolution, especially in growth and survival of neoplastic cells at both primary and secondary sites.

Thus, the framework of the study could be set to investigate the mechanistic implications of NALP3 in tumor-host interactions, in particular in the metastatic process. To appropriately study the influence of the NALP3 knockdown immune system, two cell lines, described below, were chosen because of their properties toward the inflammatory context. Concerning growth and metastasis, while LLC-B6 cells are hardly disadvantaged in a NALP3 knockdown context compared to the wild-type one, B16-F10 melanoma cells growth and propagation is severely impaired upon injection in NALP3 knockdown mice. This difference could be exploited in order to further determine what component of signaling cascade represents a targetable point in the pathway.

More specifically, these two types of cells were used to perform different *in vitro* assays. First of all, expression levels of different specific genes were assessed in both tumor cell lines, as well as in macrophages of different NALP3 genetic background. These analyses led us to further investigate the role of IL-1R1, since both tumor cell lines expressed very different level of this receptor. The hypothesis of the implication of this receptor in the promotion or not of growth and metastasis was assessed. The knockdown but also the overexpression of this receptor on tumor cells was realized using standard cloning techniques. It allowed further *in vitro* and *in vivo* tests.

In another experiment, co-cultures of tumor cells and macrophages of different NALP3 genetic background were performed to assess the profile of gene expression of both cell lines and of macrophages, using microarrays. Furthermore, laser capture microdissection allowed precise extraction of total RNA of B16-F10 metastases from lungs of either NALP3 wild-type or knockout mice. The purpose of this experience is to elucidate adaptation mechanisms of the tumor cells being in contact with two different inflammatory contexts, by performing microarrays analysis. Extracted material could also be used to study differential expression of miRNAs regarding inflammatory context, using standard RT-qPCR techniques.

3. MATERIALS AND METHODS

3.1 Cell lines used

Melanoma cell line: B16 –F10

The B16-F10 cell line is a murine melanoma of C57BL6 origin. Upon injection in syngeneic immunocompetent hosts, these cells establish metastases at different sites as for instance lungs and liver. These are thus widely used to study mechanisms of metastases propagation and other features of tumor migrations. Morphologically, the tumors and metastasis formed are more compact and rounder than in the case of LLC-B6 cells, described below, and fully adherent in culture. Moreover, these cells are easy and convenient to culture, being extended quite rapidly and not demanding special culture conditions. A standard medium is used, composed of Dulbecco's modified Eagle's medium (DMEM) with 4.5% glucose supplemented in FBS (10%), NEAA and P/S (1% each), put at 37°C in a humidified atmosphere of 95% air and 5% CO_2.

This cell line was chosen in this study because of their dependency on the inflammatory micro-environment: there are evidences (from previous studies assessed in our lab) that in a normal inflammatory microenvironment, B16-F10 metastases can propagate with ease, while in a NALP3 knock out context, with much less mature IL-1β present in the stroma, their propagation is severely impaired. These results concord with previous studies explained in the introductory part [25, 26].

Lewis Lung Carcinoma cell line: LLC–B6

The Lewis Lung Carcinoma cell line was discovered by Dr. Margaret Lewis in 1951 in the same mouse background C57BL6. Appearing like a semi-firm homogenous mass, they form widespread and highly invasive tumors and metastasis well disseminated all around the lung. Morphologically, they are semi-adherent in culture dish, smaller in size compared to other cells such as B16-F10 and require standard cell culture medium. This cell line is also widely used as a transplantable murine carcinoma to provide a model for the study of early events during metastasis development [36].

LLC-B6 were chosen to be used in the study because basically these cells are opposed to B16-F10 in terms of dependency on immune system. Their metastases were quite independent of the inflammatory context, may it be from immune system itself or even its activation. In a context of deficient Il-1β secretion as in the case of a NALP3 knockout mouse, these cells were still able to metastasize, even if slightly less than in the wild type case.

These two cell lines are thus very different in their mode of propagation, regarding the inflammatory context. This is why we reckon it could be interesting to asses both types of cells in different experiment, playing with the genetic background governing the inflammatory response in in vivo experiments.

Macrophages

Macrophages, white blood cells resulting from differentiation of monocytes, are important immune cells that function in both lines of defense: innate and adaptive immunity. Having a main role of phagocytosis through ingestion and digestion of pathogens or cellular debris, these cells also secrete different factors like cytokines such as Il-1β that stimulate and attract other immune cells. Basically, they represent the standard and first immune cells encountered as soon as an immune response has to be hired. That is why we choose these cells to kind of mimic the inflammatory context, and moreover because these are the main cells secreting the pro-inflammatory cytokine involved in our genetic model, the Il-1β. To induce the cell activation and secretion of cytokines, it was demonstrated that different PAMPS work very well, such as LPS and/or ATP [34].

Practically, macrophages can be freshly extracted from mice following specific guidelines. Because under normal conditions, the number of macrophages that can be extracted in the peritoneum is quite low, an irritant is necessary to engender a local inflammation and a recruitment of immune cells. To do so, 1ml of heated thioglycolate 3% in distilled water is injected intraperitoneously. This chemical irritant will thus induce an immune response with attraction and differentiation of monocytes. 4 days later, few millions macrophages can be harvested per mouse: the mice are sacrificed and 2ml of cold (4°C) PBS (Phosphate Buffer Saline) is injected directly into the peritoneum. The contrast of temperatures induces the detachment of macrophages from tissues and the solution enriched in immune cells can then be retrieved. After 3-4 washes like this, recovered liquid is centrifuged and an erythrolysis is performed using a hypotonic solution. Macrophages are then selected through their strong adhesion ability: 2 hours incubation in RPMI-1640 medium, ATB-ATM (1%), and Hepes (1M) allows these cells to adhere to the culture plate. The supernatant is then changed, removing all cells that did not attach, and the complete medium is added, supplemented in 10% Heat-Inactivated (HI) FCS, gentamicin (0.1%), non-essential amino acids (1%) and β-mercaptoethanol (0.035%).

In the present study, mouse peritoneal macrophages were used in vitro in order to kind of mimic the inflammatory microenvironment through secretion of cytokines such as Il1-β. Different molecules known to induce the formation of NALP3 inflammasome were used in order to check the possible activation of macrophages and to induce their secretion of these cytokines:

- LPS: lipopolysaccharides functioning in the outer membrane of Gram-negative bacteria and acting as an endotoxin, is a PAMP known to elicit a strong immune response [34]
    - Added at a concentration of 1mg/mL for 18h
- ATP: adenosine triphosphate, being the coenzyme used as an energy carrier in the cells, that, when present in the extracellular matrix, can also induce activation of macrophages [35]
    - Added at a concentration of 1 mg/mL for 30 min precisely

3.2 Techniques Used

IN VITRO TECHNIQUES

Co-cultures

In order to model the inflammatory microenvironment, we decided to co-culture tumor cells with activated macrophages. The Transwell inserts (Corning) allow co-culturing two cell lines in the same well by the use of an insert forming the upper compartment (Fig. 8). The thin polycarbonate membrane at the basis of this insert is permeable to soluble secreted factors and not to cells (0.4μm pores): only secreted molecules are able to cross the membrane and act on tumor cells.

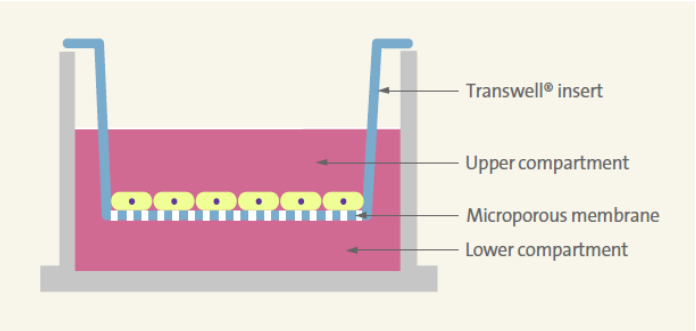

Figure 8 : Depiction of Transwell inserts used[2]

Tumor cells were grown in the lower compartment while the macrophages were put in the insert. It is basically a good standard model, especially convenient for RNA extraction, since the two cell populations are not mixed. However, the main drawback is the fact that the cells are not in direct contact as in the real context, changing and thus lacking all the contact interactions and reactions.

Macrophages from both background, NALP3 KO or WT, were used to compare both conditions. Briefly, 150 000 freshly extracted macrophages were seeded and, after 2 hours required for attachment, the medium was removed and washed 2 times with PBS and 200μl of the complete macrophage medium was added. At the same time, the same number of tumor cells is seeded in the lower compartment. 8 hours later, the LPS and/or ATP were added as described for 18h or 30minutes, respectively, in order to activate the macrophages and induce the normal inflammatory response, therefore mimicking the inflammatory context. Both type of cells, tumor cells and macrophages, were recovered thereafter using different lysis buffer in order to extract total RNAs and supernatant was kept to perform Western Blot analysis.

RNA isolation

Extraction

RNA extraction was performed differently regarding the quantity of cells available. For the co-cultures where the number of tumor cells was sufficiently high (500'000 cells) to use a

standard kit, the RNeasy® Mini Kit was chosen, appropriate for micrograms of RNA. For the macrophages in co-cultures, since their number was much lower (150'000 cells) because of their nonproliferative state, and for the tissue samples extracted with laser capture microdissection (see below), the RNaqueous Micro Kit was more suitable since it is optimized for recovery of total cellular RNA from pico-samples. In both cases, RNA extraction was performed according the manufacturer's instructions:

RNeasy® Mini Kit Protocol (Qiagen)

First, a lysis buffer containing β-mercaptoethanol is applied to the cells, pelleted or in the wells, for membrane disruption and RNases inactivation. The obtained lysate is then homogenized by passing through a spin column that removes all undisrupted elements. The addition of ethanol is then used to provide optimal binding conditions to the silica-based membrane for the second spin step, carried out to allow total RNA to attach to the silica-based membrane. Finally, different washes are made to remove other contaminants from the membrane and RNase Free water is applied directly to the spin column to elute RNA.

RNaqueous® Micro Kit Protocol (Ambion)

This kit is optimized for extraction of RNA from micro sized samples: 10 mg of tissue or even 10 microdissected cells are sufficient. The other specialty is the filter cartridge that is designed specifically for very small samples.

In a few words, it uses a powerful chaotropic guanidinium thiocyanate solution to solubilize samples: it effectively lyses cells and inactivates endogenous ribonucleases. Ethanol is then added to dilute the lysate: this step offers the possibility to extract both large and small RNA species as tRNAs, rRNA, and microRNAs or only large RNAs. Then, the mix is applied to an RNA-binding glass fiber filter and three washing steps remove proteins, DNA and other contaminants. Finally, the bound RNA can be eluted and concentrated in a minimal volume of 20 µl. The kit also offers the possibility to remove genomic DNA by using the DNA-free system[2].

Quantity and purity determination

RNA quantity and purity were assessed with the NanoDrop® ND-1000 spectrophotometer of NanoDrop Technologies Company, USA.

This spectrophotometer measures absorbance of a solution: a pulsed xenon flash lamp provides light source of given wavelength, this light passes through the solution and is collected in a spectrophotometer that analyzes it thereafter.

Briefly, the Beer-Lambert equation describes this phenomenon: the correlation of the absorbance of the solution with the concentration of substances in this solution, at wavelength at which these absorb light. Note that this instrument, with full-spectrum from 220 nm to 750 nm, is able to measure very small samples (1 µl) with very high accuracy, a good point since it enables to minimize loss of samples. Mathematically, it is as follow:

[2] RNaqueous Micro Kit GUIDE: http://www.ambion.com/techlib/prot/fm_1931.pdf

$$\boxed{I = I_o\, e^{-\epsilon LC}}$$ **Beer's Law**

Where: I and I_o = Intensity collected and intensity emitted

C= concentration [mol / L]

L = length of the optical path [cm]

ε = molar absorptivity , in function of wavelength [L/mol/cm]

and to find the concentration we get: $$\boxed{C = \frac{-\ln\left(\frac{I}{Io}\right)}{L\,\epsilon}}$$

The other two main indications we get from these measurements are the 260/280 and 260/230 ratios. Those are used to evaluate the purity of RNA or DNA. Concerning here RNA, the solution is received as pure if the 260/280 ratio is around 2. A lower number would indicate presence of contaminants such as proteins or phenol absorbing light near 280nm. The 260/230 ratio has to be between 1.8 and 2.2, and co-purified contaminants would also lower this number.[3]

RNA precipitation

After measurements with the NanoDrop, the samples were precipitated in order to remove all contaminants. The following procedure was very helpful in removing all contaminants. Moreover, the both ratios were then around 2, indicating pure RNA samples.

The successive addition of 3M NaOAc pH 5.2, EtOH and glycogen with 2 hours at -80°C for precipitation was followed by 30 minutes of centrifugation, 2 washes with cold 70% EtOH. The pellet is air dried 10 min before to be resuspended and re-concentrated in nuclease-free H2O to yield desired concentration.

RNA quality control

After having performed the extraction and purification of the totRNA, the quality control was made at the UNIL DAFL facility: they used the Agilent 2100 Bioanalyzer of Agilent Technologies.

Basically, the RNA 6000 Pico kit used with this technology takes the advantage of microscale format to determine the quality of a sample. Moreover, only very small amount of samples are required in order to perform the analysis. After the analysis, the bioanalyzer is able to represent the data on an electropherogram, accompanied with a gel-like image that facilitates the representation of the samples' quality (Figure 9). A good quality totRNA will be represented on the electropherogram by two ribosomal peaks, the 18S and 28S and the ratio of 28S/18S peaks should be higher than 2. In the case presented in Figure 9, the totRNA presents some degraded RNA: the additional peaks represents shorter RNA fragments that have the tendency to decrease the ratio below 2.

[3] Nanodrop User Manual, p-27-30 : http://www.nanodrop.com/Library/nd-1000-v3.7-users-manual-8.5x11.pdf

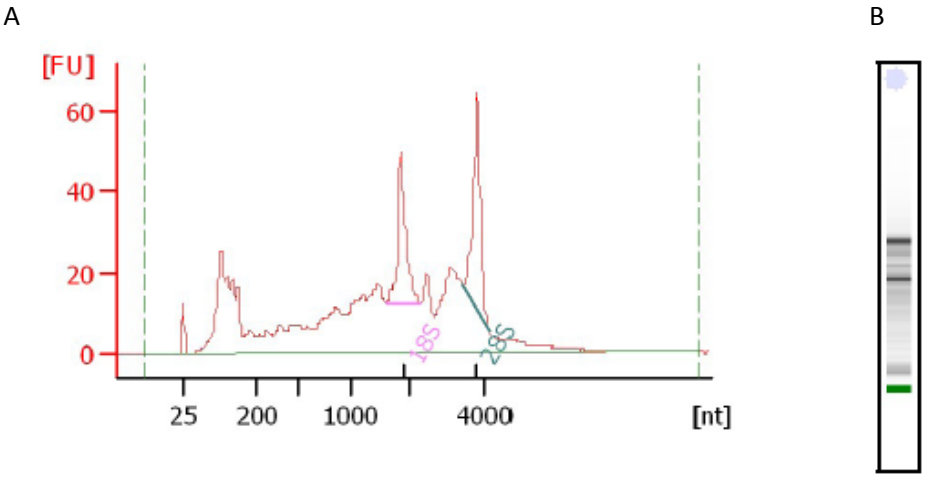

Figure 9: (A) Example of an electropherogram obtained from the bioanalyzer **(B)** Example of the gel-like image corresponding to the electropherogram. The 18S and 28S peaks represent the ribosomal mRNA peaks, also present on the gel image: the two upper darker bands: at 1.9 kb for the 18S peal and at 5.9 kb for the 28S peak

RNA amplification

The amount of RNA extracted from macrophages and LCM samples was quite low (between 150-170 ng) and the minimal amount required to perform microarrays is 12,5 µg. In order to have enough material to perform both Affymetrix microarrays and qPCRs thereafter, it was decided to amplify the starting material with the Ovation Pico WTA System from NuGen technologies.

The advantages are that the amplification is initiated both at the poly(A) tails but also randomly throughout the whole transcriptome so that the coverage is complete[4]. This allows analyzing both degraded or partially compromised RNA samples and non-poly(A) transcripts. The amplified product is also optimized for analysis on Affymetrix GeneChip arrays.

This system is based on the Ribo-SPIA technology from NuGen, in which a rapid, simple and sensitive RNA amplification is made following a three-step process that generates amplified cDNA in microgram quantities. In brief, the 3 steps are (Figure 10):

1) The first step is the generation of the first strand cDNA: Reverse transcriptase and DNA/RNA chimeric primer mix allows the 3' DNA end of each primer generating first strand cDNA. It results an mRNA/cDNA hybrid molecule containing a unique RNA sequence at the 5'end of the cDNA strand.
2) Then, the fragmentation of the mRNA within the hybrid molecule creates the priming sites so that the DNA polymerase can elongate the second strand. The double strand cDNA is generated, still containing a hybrid RNA/DNA end.
3) Finally, the SPIA amplification takes place: the DNA is amplified linearly and thus the difference in their expression levels is maintained. In this reaction, successive steps are repeated: SPIA DNA/RNA primer binding, DNA replication, strand displacement and RNA

[4] http://www.nugeninc.com/tasks/sites/nugen/assets/File/user_guides/userguide_pico_wta.pdf

cleavage by an RNase. This lead to a rapid accumulation of cDNA: these molecules have the complementary sequences to the original mRNA.

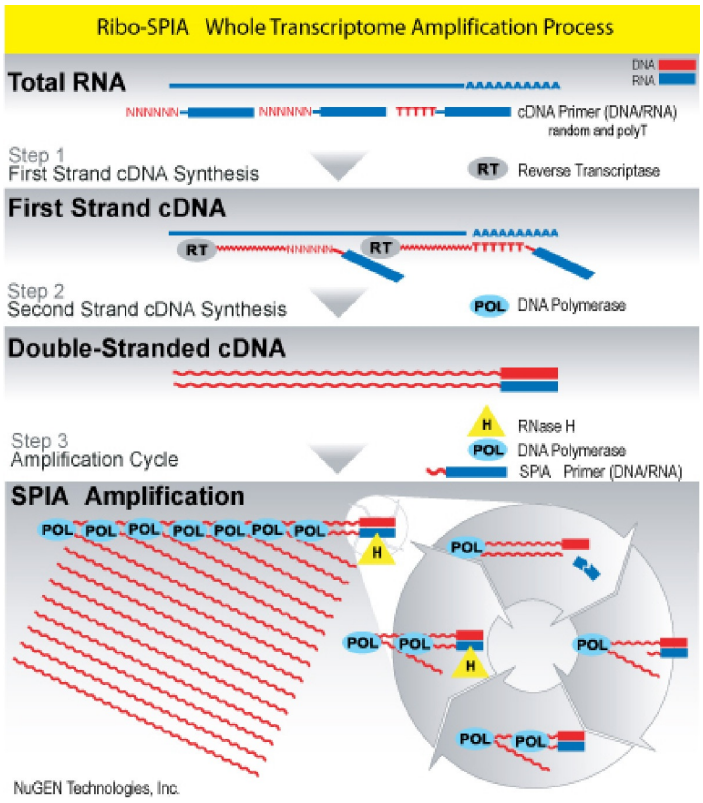

Figure 10: The Ribo-SPIA RNA Amplification Process used in the Ovation Pico WTA System[5]

RNA fragmentation and labeling process

To further hybridize samples to Affymetric GeneChip Arrays, the obtained cDNA has be to fragmented and biotin labeled to generate targets that are suitable for arrays hybridization.

These steps, performed at the DAFL, were performed using the Nugen Encore™ Biotin Module[6]. The fragmentation combines a chemical and enzymatic process to generate a single-stranded cDNA in the 50 to 100 base range. In the next step, the obtained product gets labeled via enzymatic attachment with a biotin-labeled nucleotide to the 3' end of the fragmented cDNA. The hybridization on microarrays can then be made.

Microarrays

The GeneChip Mouse Gene 1.0 ST Array (Affymetrix) was used to determine the gene expression profile of the different samples. It offers whole-transcript coverage in which the 28'853 genes are represented by approximately 27 probes spread across the full length of the gene. This provides a complete and accurate representation of gene expression[7].

[5] http://www.nugeninc.com/tasks/sites/nugen/assets/File/user_guides/userguide_pico_wta.pdf
[6] http://www.nugeninc.com/tasks/sites/nugen/assets/File/user_guides/userguide_encore_biotin.pdf
[7] http://www.affymetrix.com/browse/products.jsp?navMode=34000&productId=131476&navAction=jump&aId=productsNav#1_1

After fragmentation process described above, the hybridization of the labeled samples could take place. The microarrays were then washed and scanned to return an output file, a CEL file, containing for each probeset a value representing the level of expression. From the CEL file, the statistical analysis could be launched, with the help of our bioinformatician, Paolo Provero.

Quantitative Real-Time RT-PCR

Reverse transcription- quantitative polymerase chain reaction, RT-qPCR, represents a very sensitive technique allowing the detection and quantification of mRNAs expression in a given sample.

First of all, mRNA is transcribed to cDNA using a reverse transcription reaction and this cDNA is the template for the quantitative PCR realized thereafter. Only specific region of the target gene gets amplified with this technique by the use of gene-specific primers or probes fluorescently labeled. The device monitors during the reaction the fluorescence emitted, a parameter that is related to the amount of product for each tested mRNA of interest. Then, since one cycle can be considered to double the number of molecules present in the solution, the user can then determine the initial quantity of RNA in the samples, relatively to a control mRNA, allowing to establish the expression level of a given gene in the present sample [18].

Practically, after mRNA extraction, 500ng of mRNA is taken for a reaction of reverse transcription in order to obtain corresponding cDNA. Random hexamers, dNTPs and reverse transcriptase were mixed following standard method with the template mRNA. Thereafter, the real-time PCR could be performed using the ABI Prism 7700 device from Applied Biosystems. SyBR green mix and TaqMan primers and probes where used for the quantification reaction. To explain briefly the mode of action of both, first the SyBR green is a double-stranded DNA intercalant. Thus it binds to the PCR product obtained after the step of amplification. As the amount of PCR product increase, the amount of bound SyBR green increases also. For the Taqman probes, the mode of action is slightly different: the probe contains at its 3'end a quencher dye and at the 5' end a reporter dye. In the unbound state, no fluorescence is emitted since the proximity of both allows the 3' end to quench the reporter. The 5' nuclease activity is exploited during the PCR reaction: it will cleave the probe so that reporter and quencher are separated and thus, fluorescence is now emitted. For every cell type an endogenous control mRNA was tested in order to normalize the level of expression of the other tested mRNAs.

Concerning the PCR cycles set up, these are the following:

	Temperature	Time
Stage 1	50° C	2 min
Stage 2 **Denaturation**	95 ° C	10min
Stage 3 **Denaturation and annealing of primers**	95° C 60° C	15 sec 1 min
Stage 3 repeated **40x times**		
Stage 4 **Dissociation Curve**	95° C 60° C 95° C	15 sec 15 sec 15 sec

The sequences of the forward (Fw) and reverse (Rev) primers and probes are:

mIL1b-FW	: 5'-TGC AGA GTT CCC CAA CTG GT -3'
mIL1b-RV	: 5'- CCA TCA GAG GCA AGG AGG AA-3'
mIL-1R1 FW	: 5'- CTG TAA ACC TCT GCT TCT TGA C-3'
mIL-1R1 RV	: 5'- TGG TTG AAG GAT GTT CCA CA-3'
mIL18 FW	: 5'-GGC CGA CTT CAC TGT ACA ACC GC-3'
mIL18 RV	: 5'-ACA GAG AGG GTC ACA GCC AGT CC-3'
mCasp1 FW	: 5'-AAG GCA CGG GAC CTA TGT GA-3'
mCasp1 RV	: 5'-AGC TCC AAC CCT CGG AGA AA-3'
mBeta Actin FW	: 5'- ATGGATGACGATATCGCTGCGCTGGTCGTC- 3'
mBeta Actin RV	: 5'- CTA GAA GCA CTT GCG GTG CAC GAT GGA GGG- 3'
mGAPDH FW	: 5'- ACCACCAACTGCTTAGCCCCCCTGGCCAA-3'
mGAPDH FW	: 5'- GGA TGC AGG GAT GAT GTT CTG GGC AGC CCC AC -3'

For the NALP3 probe, the sequence is unknown since AB is selling it ready to use and specifically for NALP3, see the reference[8]. The same stands for the miRNAs primers sequences that were ordered on the Exiqon platform for the following miRNAs: miR-21, miR-140, miR-155, miR-181, miR- RNU-g and U6 as reference miRNAs[9].

Western blotting

This technique allows specific identification of proteins by the use of corresponding antibodies. Basically, the proteins are separated according to their size through gel electrophoresis. The gel is then put in contact with a membrane made of nitrocellulose. Thanks an electrical current applied to the assembly, the proteins contained in the gel are transferred to the membrane so that the latter becomes a replicate of the gel's pattern. This membrane can then be stained with Ponceau Red to detect the presence of proteins and then it is blocked with milk so that the specific antibodies can be applied to target accurately the protein of interest. This can then be detected using specific development methods.

Practically the method is as follows:

1. The proteins are extracted using a specific lysis buffer. The supernatant of cell culture can also be used. In our case, the lysis buffer used is composed of: 50mM Tris HCl pH7.4, 150mM NaCl, 1mM EDTA, 1% Triton X-100 and proteases inhibitors. The dosage of proteins is then made using the standard Bradford method (Bio-Rad Protein Assay). To determine the correct concentration of proteins, a reference range is made using BSA.
2. The proteins extracts are then denaturated 5 minutes at 100°C in the loading buffer. This buffer is composed of: 10mM Tris, 6,9% SDS, 15% β-mercaptoethanol, 30% glycerol, 5% bromophenol blue.
3. The gel electrophoresis can then be run. The gel is composed of two stacks: at bottom the running gel allows separating proteins according to their size and above the stacking

[8] https://products.appliedbiosystems.com/ab/en/US/adirect/ab?cmd=ABAssayDetailDisplay&assayID=Mm00840904_m1&Fs=y&SearchRequest.Common.PageNumber=1&assayType=ge&chkBatchQueryText=false&srchType=keyword&searchValue=nlrp3&searchBy=all&msgType=ABGEKeywordResults

[9] http://www.exiqon.com/mirna-pcr-primer

gel provide an environment concentrating the proteins, creating a thin starting zone. The composition of gels is standard.

4. After the electrophoresis, the gel is taken out and put in contact with a nitrocellulose membrane so that the transfer of proteins contained in the gel to the membrane can occur.
5. After 2 hours of transfer, the membrane is recovered and rinsed with TBS solution. Red Ponceau is put then to color basically all the proteins present on the membrane. This color is washed several times with TBS and then the blocking of aspecific sites is realized with a solution containing 5% Regilait, 10% TBS and 0.1% Tween-20. 3 washes are necessary before to put the primary antibody overnight. For the exact dilutions of antibodies used, see the following table. Again, 3 washes are made before to put the anti-α-tubulin antibody for 1 hour. After washes, the membrane is incubated 1 hours with a mix of secondary antibodies that are Horse-Radish-Peroxidase (HRP)-conjugated.
6. The final step is the rinsing and the revelation is made by chemiluminescence. The substrate of the HRP is added on the membrane and incubated according to the manufacturers' instructions[10]. The SuperSignal West Pico and Femto kits from Thermo Scientific were used. Then, the blots are exposed to film for 30 seconds or one minutes exposures, depending on the signal obtained.

The antibodies used were as follows:

Antibody		Dilution used
Rabbit anti-IL-1β	Abcam	1/3'000
Mouse anti-α-tubulin	Abcam	1/4'000
Rat anti-IL-1R1	R&D Systems	1/500
Anti-mouse antibody HRP-conj.	Dako	1/20'000
Anti-rabbit antibody HRP-conj.	Dako	1/10'000 & 1/20'000

CLONING STRATEGY

Silencing and overexpression of the Interleukin 1 Receptor type I - Il-1R1

In order to study the importance on metastasis capability of the IL1-RI, overexpression and silencing of this receptor on the surface of the cells of interest was to be studied. We had to design a specific protocol for each cloning strategy, since it involves *in vitro* preliminary tests and further *in vivo* studies.

SILENCING

Since the silencing should also be efficient for further *in vivo* studies, it was decided to use a small hairpin RNA, shRNA, therefore inducing a stable and long-term silencing of the target mRNA.

[10] www.piercenet.com/instructions/2160683.pdf

Stable transfection

This kind of RNA, designed as a tight hairpin turn, works via RNA interference: it uses a vector that gets introduced into the genome of cells. The shRNA is under the regulation of the U6 promoter that will ensure its expression to be constitutive in the target cells.

The shRNA is processed by the cellular machinery so that it can bind the RNA-induced silencing complex, RISC. The cleavage of the target mRNA is then made by the complex of both molecules, leading to proteasomal degradation or translational repression.

Technically, the RNAi-Ready pSIREN was used as a vector, in which we introduced the shRNA targeting the Il1R1. The selection of the target sequences is very important in order to correctly match the mRNA of interest and be efficient in the repression. Different criteria have to be fulfilled during the selection and at least 2 shRNAs per gene have been designed, since most of the time, one of them works better than the other one and also to be sure that the observed changes are really due to the sh and not to an artifact. Moreover, a control sh molecule is required: this one is designed so that it is a scramble of the "active" sh, meaning that it should not bind at any region of the gene. It is required so that the cells of interest also undergo the same protocol and selection procedures as the one with the active sh.

The sequences taken for the silencing and introduced in the pSIREN vector are the following:

- mIL-1RI shRNA 762 : Top Strand (66bp)

5'-gatccGCGGTCACACGAGTAATACATTCAAGAGATGTATTACTCGTGTGACCGTTTTTTACGCGTg-----3'

- mIL-1RI shRNA 916 : Top Strand (66bp)

5'-gatccGCTGGAAGTGGAATGGATCATTCAAGAGATGATCCATTCCACTTCCAGTTTTTTACGCGTg-----3'

-mIL-1R1 shRNA shCTL: scramble molecule: Top Strand (66bp)

5'-gatccGGTTTAGGGTCATTCTATAGTTCAAGAGACGCTTGTATCGTTGTAATAGTTTTTTACGCGTg----- 3'

Beside the shIl1R1 that targets the most efficiently the mRNA encoding the Il-1R1 protein, sh762, the sh916 was less efficient but we used it in all the experiment made. The control-scramble sh is called in the rest of the report as the shCTL.

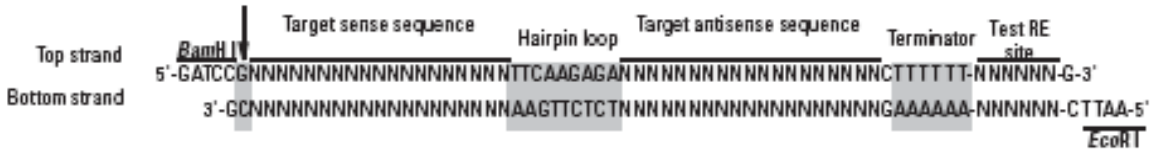

Figure 11: Schematic representation of shRNA [11]

The procedure to obtain tumor cells transfected with the shIl1R1 is then the following (Figure 12):

- The first step was to ligate the annealed double-stranded oligonucleotide into the RNAi-Ready pSIREN, the latter being previously digested with BamHI and EcoRI in order to get an empty vector, ready to welcome a new sequence.

[11] http://www.clontech.com/images/pt/dis_manuals/PT4055-1.pdf

- The next step is to transfect bacteria (E.coli DH10) by electroporation, so that we could select those bacteria being positive for the plasmid thanks the ampicillin resistance the introduced vector confers.

- Different steps are then required to verify that the RNAi sequences are really in the plasmid: miniprep for recuperation of the plasmid, digestion with MluI and electrophoresis migration in order to check the right linearization of the plasmid and finally sequencing reaction. If the sequence is correct and the vector contains the desired sh, the plasmid gets amplified via bacterial culture and gets extracted with a maxiprep.

- GP2 cells are then used because of their ability to produce retroviruses. By mixing a given plasmid encoding for the envelope of the VSV virus, the plasmid of interest, pSIREN containing shIl1R1, and FuGENE, a reagent that helps to cross cell membrane, we get micelles that are ready to enter the GP2 cells. After incubation, GP2 produce enough viruses in the supernatant. The latter is filtered and used to do two rounds of infections on the cells of interest, in our case: B16-F10 and LLC-B6 tumor cells.

- The final step is then to select the cells having correctly integrated the virus and thus the sh of interest with at least 4 rounds of selection with the drug-resistance marker included in the transfected DNA, puromycin in this case.

OVEREXPRESSION

The overexpression of the Il1r1 gene was carried out using the pMM34 plasmid. In this plasmid, the promoter sitting in front of the introduced target gene is also expressed constitutively.

The first step of the procedure was to isolate a template from a given library of murine cells: taking primers on the mRNA of the transcript variant 1 of Il1R1, we could isolate the mRNA sequence of Il1R1 of 1962 bp in order to clone it into the pMM34 vector. The primers used to do so are the following:

For the forward primer, it has to introduce the restriction site for further cloning in pMM34, the PmeI site (in blue):

Primer Forward 1:

5' – ACGTTTAAACTGAGCTGTCTGTCATTCTTG– 3'
PmeI Fw

Concerning the reverse primers, two primers were used so that, beside the introduction of the second restriction site required for cloning into pMM34, a V5 tag was introduced, allowing further specific protein isolations. Two steps of amplifications were thus required to introduce both:

Primer Reverse 1:

5' – **CGCGTAGAATCGAGACCGAGGAG**AGGGTTAGGGATAGGCTTACCGCCGAGTGGTAAGTGTGT- 3'
v5 Part1 Rv

Primer Reverse 2:

5' - TATCATATGTCAATGGTGATGGTGATGATGACCGGTA**CGCGTAGAATCGAGACCGAGGAG** - 3'
NdeI v5 Part2

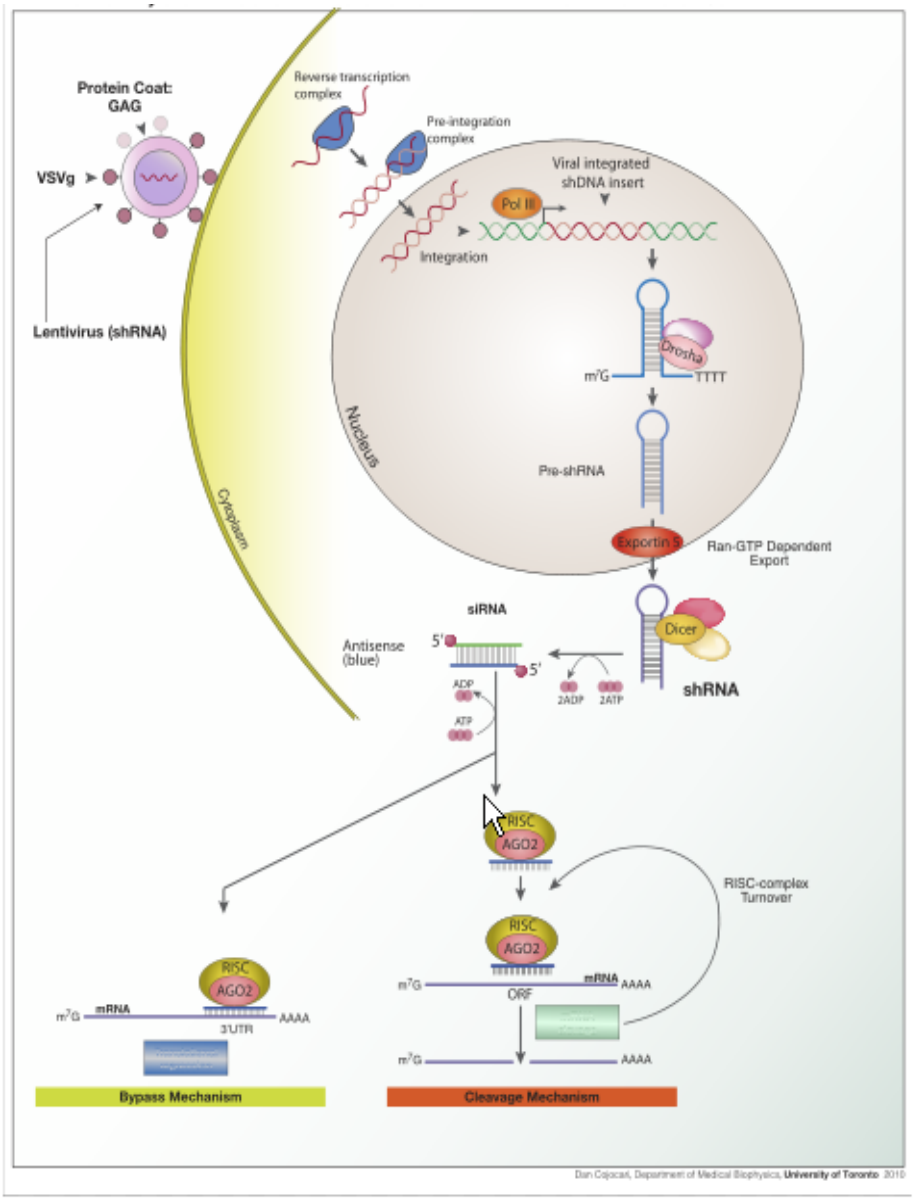

Figure 12: Lentiviral delivery of shRNA and mechanisms of RNAi interference in mammalian cells [12]

In the design of the plasmid, the mRNA sequence of the Il1R1 was taken since we only need this sequence to get the protein expressed. Since the mRNA sequence is shorter than the gene itself, it renders the cloning easier.

Moreover, concerning the drug-markers used, it was interesting to use 2 different pMM34 plasmids: one, pLIV puro, contains the puromycin resistance cassette and the other one, pLIV hygro, contains hygromycin resistance gene. The reason is because of the target tumor cells: the B16- F10 cells were also previously modified so that they express luciferase and this cloning was made using the puromycin resistance gene, so that, on these cells, another infection with the same antibiotic

[12] Dan Cojocari, Department of Medical Biophysics, University of Toronto, 2010, http://upload.wikimedia.org/wikipedia/commons/thumb/e/e4/ShRNA_Lentivirus.svg/640px-ShRNA_Lentivirus.svg.png

selection would not be representative. Thus, having a second selection cassette for the introduction of the overexpression allows the B16-F10 luciferase-expressing cells to be infected with the overexpression plasmid, for an eventual *in vivo* experiment.

This sequence was then amplified using the high-fidelity polymerase Phusion Hot Start Enzyme, The PCR required 2 steps, one with the forward primer and the reverse 1, one with the same forward primer and the second reverse one. Different set-ups were necessary in order to correctly isolate the mRNA of interest. After verification and purification of the right sequence with gel electrophoresis, the digestion of the PCR product and the pMM34 receiver plasmid was realized with PmeI and NdeI. Both products were isolated on a 1% agarose gel and purified so that the ligation could then take place.

The rest of the procedure basically remains the same as for the silencing: electroporation in electrocompetent bacteria, selection, amplification and extraction of the plasmid of interest, followed by transfection thanks retrovirus in GP2 cells and finally infection of target cells.

Finally, the whole sequence on the plasmid was sequenced in order to check for mutation during the cloning process. Here the primers used cover the whole sequence. These were designed using Clone Manager and are the following:

Forward	**Reverse**
FWD 1: 5'-TTTGTCTCATGGTGCCTCTG-3'	
FWD 2: 5'-CCGAGGTCCAGTGGTATAAG-3'	REV 3: 5'-GGGCCAGTTCTCAGACCTTG-3'
FWD 3 : 5'-TTGAGTCGGCGCATGTGCAG-3'	REV 4: 5'-TGGAGGGACAGTTTGGATAC-3'
FWD 4: 5'-TGGGCCAGTCATCTGAAGAG-3'	REV 5: 5'-TACCGGTCATCATCACCATC-3'
FWD 5: 5'-CCGGTCATCATCACCATCAC-3'	

Proliferation Assay

Proliferation is an important factor to assess when a genetic modification is introduced in a cell, to see the influence on survival and proliferation it can induce.

In this case, the Cell Titer 96® Assay was used. The assay is based on the cellular reduction of yellow MTT, a tetrazole, into purple formazan, a reaction taking place in mitochondria of living cells. The advantage is that the absorbance of the colored solution is easily quantified by measuring it at a given wavelength, usually between 500 and 600 nm, by a spectrophotometer. The idea is that this reaction occurs only when mitochondrial reductase enzymes are active. Therefore, the conversion is directly proportional to the number of viable and living cells[13]. The drawbacks of this technique are the followings: first, the physiological state of cells can influence the enzymatic activities, and second there can be differences in mitochondrial dehydrogenase activity with different cell types.

Practically, same amount of cells are plated (5000 cells in a 96 well plate), including the appropriate controls. After 24h of incubation, the Dye Solution is added to the medium for 4 hours. During this time, the living and metabolically active cells convert the tetrazolium component of the dye solution into formazan. Then, a stop solution allowed solubilizing the formazan product: the more the formazan product, the more the cells are metabolically active, the more the proliferation. The absorbance at 580nm is read using a plate reader. Proliferation levels can then be established

[13] http://www.mnstate.edu/provost/mtt%20proliferation%20assay%20protocol.pdf

and compared between the different sets of cells, subtracting the average absorbance of the no-cell control wells.

Migration Assay – Wound Assay

This assay is carried out to estimate the migration rates of the different cells used and/or different conditions introduced. Concerning cancer cells, it is a very interesting parameter to determine since wound healing involves complex series of events that most tumor cells are able to control. Provoking a wound in tissue culture can re-activate some cascade that are important for a given cell type in order to increase proliferation or extracellular matrix deposition[14].

Basically, using a confluent cell monolayer, a small area gets disrupted by scratching a line through the layer. This gap is then followed microscopically and the migration, if it happens, can be inspected. This "healing" can be rapid, over several hours as well as taking few days, depending on the cell type but also conditions of culture and the extend of the scratched region.

Practically, cells are cultured in 48-wells plate and, at confluence, the wound is realized with a tip under the hood. The movement has to be precise and straight. Then, the dead and detached cells are rinsed with 2 washes with PBS and then the normal culture medium is added. Every 24 hours a picture is taken, making a mark on the cap of the plate to stay every time at the same position. Such pictures are taken at a magnification of 10x, but taking some at 20x magnification can be very interesting in terms of morphology. The latter point at the leading and trailing edge of the cell can show different parameters of cell migration.

Soft Agar for Colony Formation Assay

This assay allows measuring the invasion potential and properties of the cells to form colonies in a three dimensional culture. The aggressiveness of tumor cells is closely linked to certain phenotypical changes such as loss of polarity, loss of contact inhibition where cells can grow over one another, and anchorage independence where cells form colonies in soft agar. Transformed cells acquired the anchorage-independent features, characteristic of tumor cells, so get the ability to grow in a viscous gel without basement membrane as support. The colony formation assay is based on the process by which these phenotypic differences can occur, mainly related to the process of *in vivo* carcinogenesis[15].

Practically, after having prepared the 0.8% soft agar base layer, the cells are mixed with medium and 0.7% agar to form a top layer. A same number of cells are prepared and each cell type is plated in triplicate. The assay is then realized over 15-20 days to test the anchorage independency in growth of the tested cells. Pictures are also taken every day, also using a mark on the cap of the plate to stay at the same position for each picture. Finally, the morphology of the formed colonies, if occurred, can be analyzed using cell stain and the number of colonies can be quantified.

[14] http://www.mnstate.edu/provost/woundAssayProtocol.pdf
[15] http://www.mnstate.edu/provost/Soft%20Agar%20Assay%20Protocol.pdf

IN VIVO STUDIES

Tumor growth and metastasis assays

Different types of cells were chosen for these assays: both types of tumor cells with down- and up-regulated IL-1R1 were taken, adding cells with a control (CTL). Cells were detached from culture plates with addition of 2ml Trypsin-EDTA, centrifuged and resuspended in a given quantity of medium so that 50'000 cells could be injected subcutaneously in 50ul for each mouse and 500'000 cells for the tail-vein injections, in 150ul. C57BL/6 male mice of 8 weeks were used for this purpose.

- For subcutaneous injections **(primary tumor growth assay)**, 6 mice were used with the following scheme:
  Mice were sacrificed 2 weeks after injection, tumors were removed, weighted and measured, and included in paraffin for later morphologic and infiltration observations.

LEFT (on the back)	RIGHT (on the back)
B16-F10 CTL	B16- F10 sh762
B16-F10 CTL	B16-F10 sh762
LLC-B6 CTL	LLC-B6 sh762
LLC-B6 CTL	LLC-B6 sh762
B16-F10 overexpressing IL-1R1	LLC-B6 overexpressing IL-1R1
B16-F10 overexpressing IL-1R1	LLC-B6 overexpressing IL-1R1

- For tail-vein injections (**experimental metastasis assay)**, 2 mice were taken for each cell types, i.e., B16-F10 and LLC-B6 and for both: sh762, overexpression of IL-1R1 and CTL. :
  Mice were sacrificed 2 weeks after injection, lungs and livers were carefully removed, visible metastatic foci were counted before to include these organs in paraffin. Micro-metastases were then counted by microscopy and the percentage of lung/liver surface colonized with metastasis was evaluated. Criteria for identification of metastases:
  - Round shape
  - Uniformly colored
  - Appearance different from surrounding normal tissue

Xenogen Bioluminescent System

After the tail vein injection of tumor cells, it is possible to monitor *in vivo* growth of metastases with a non-invasive bioluminescent measuring device, using the Xenogen IVIS System. This device quantifies single-photon signals originating within the tissue of living mice, thanks to the *luciferase* gene previously introduced in tumor cells genome.

Briefly, this enzyme oxidizes its substrate, the luciferin, to produce an oxidized substrate, oxyluciferin, and energy in form of light, responsible for photon emission. The minor disadvantage is that the luciferin has to be intraperitoneously injected just before each imaging session. Moreover,

from that point, the maximum photon emission signal is reached during the first 10-12 minutes so that the signal has to be monitored every two minutes until the signal goes down.

Technically, this device is composed of a light-tight imaging chamber, coupled to a highly-sensitive CCD camera system, an optical filter wheel and an acquisition computer. The Living Image Software provides an interface for imaging and data collection. The imaging chamber consists of a housing chamber in which up to five mice can be placed for imaging and a heated and moveable platform. The mice are maintained under temporary anesthesia thanks an integrated isoflurane gas manifold.

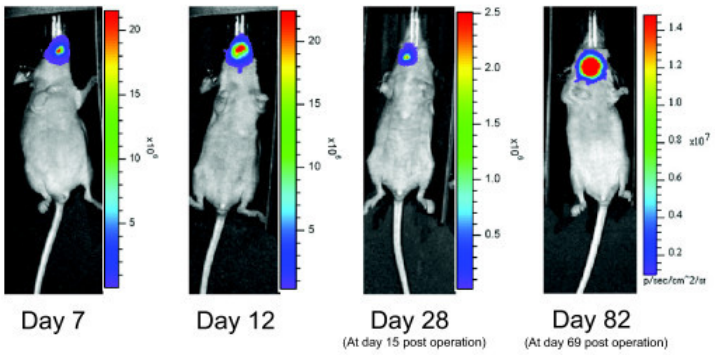

Figure 13: Bioluminescence imaging of mice orthotopically transplanted with luciferase-transduced cells[16]

Organ extraction and sample handling

The tumor cells chosen for these studies are quite aggressive and could establish metastases at different locations rapidly given the genetic background. That's why, the wild type mice were sacrificed 20 days after the tail vein injection, instead of 23 days for the NALP3 KO mice: since the B16-F10 are not so fit in establishing metastases in such down-regulated inflammatory background, we waited until a same late stage signal on the xenogen was obtained to sacrifice them.

At this point, the most important is to conserve the quality and integrity of the RNAs, easily degraded by RNases: the extraction of organs from mice has to be very fast. The lungs and livers were thus directly put in liquid nitrogen and kept all the time at -80°C. A cryostat was used to cut 14µm thick frozen tissue sections, directly used for laser capture microdissection.

Microdissections assisted with the laser capture: Laser Capture Microdissection LCM

Laser assisted microdissection allows isolating precisely specific cell populations from microscopic regions of tissue samples.

In this case, the µCut Laser Microdissector System (Nikon) was used in order to isolate specific samples of B16-F10 tumor cells. Indeed, these cells established metastases in the lungs of wild-type and NALP3 KO C57BL6 mice.

[16] http://www.biomedsearch.com/nih/Xenograft-models-head-neck-cancers/19678942.html

The device is composed of an inverted microscope (Nikon Eclipse TE200) equipped with a motorized scanning stage assisting the CCD camera coupled to the computer. A laser and an optical-electronical coupling unit also belong to the system. The associated software, µCut software (V 1.01, SL Microtest), allows the user to precisely focus on the desired regions of the samples and to examine the nature of the given cells, since the camera is coupled to the objective and transfers the images of the histological sections to the computer. Moreover, the software contains precise drawing tools used to encircle cells or populations of interest with high accuracy and precision in the cell-scale.

Here is a brief description of the whole procedure. After mounting the frozen tissue sections on the polyvinyl membrane of the special LCM slides, the tissue sections are fixed, stained and dehydrated following a defined protocol. Three ethanol baths of 95%, 70% and 50% allow fixing of the tissue and dissolution of the organ embedding gel. Then toluidine blue (1% in DEPC water and 0,45 µm filtered) is used to stain the cells. This dye is simpler to use than hematoxylin-eosin stain and also quicker. Moreover, only one dye is required to color different cellular component in a metachromatic way. DEPC water is important in this process since it is water in which all RNases are inactivated by the addition of 0.1% of diethylpyrocarbonate (DEPC) to deionized water, incubated overnight and autoclaved. Ten seconds are required to stain the tissue sections and then 3 baths in DEPC water rinse the slide. Finally 30 seconds in 70% EtOH are required to dehydrate the samples, a crucial step in the procedure since residual moisture would enhance hydrostatic forces making the sample more difficult to separate from the slide and surrounding tissue. Thereafter, the slide is placed on the microdissector system using a glass slide as support. The user can then visualize the slide and predefine a track along which the laser has to cut, without radiating the selected cells. After the cut, a special collection tube is used: it contains a compact lid with specific adhesive properties. When it is placed on the dissected samples, the latter get trapped by the cap. The whole cutting process has to be done in 20 minutes to preserve the RNA integrity. Then, the lysis buffer of the RNaqueous® Micro Kit is added and put 30 minutes at 42°C and can be freezed for further sample processing. Total RNAs were extracted from the samples (as described above) in order to proceed to microarray analysis.

A

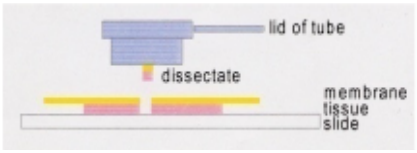

B

C

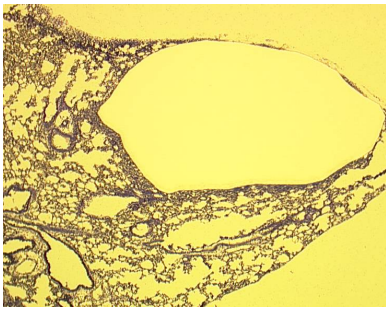

Figure 14 : (A) scheme depicting the arrangement of the LCM slide on the glass support and the position of the tissue in between. Example of microdissection of a lung section placed on the membrane of a LCM slide. (**B**)

Section before the removal of the microdissected tumor region, (**C**) after the cut and removal of the area of interest with the lid of the cap / Magnification : 100x

Extraction of macrophages from tumor microenvironment

B16-F10 cells were tail vein injected, 500'000 cells/mouse, into 2 WT and 2 NALP3 KO female mice. See section "Assay of metastasis" for cells preparation. After 2 weeks, mice were sacrificed and lungs and ovaries of these mice were extracted so that macrophages in contact with tumor niches could be isolated. The ovaries of mice were also taken since they were bigger than normally, suggesting a possible strong infiltration of tumor cells.

Concerning the extraction protocol, it is as follows:

1. A collagenase solution made of Collagenase II (Sigma), Collagenase IV (Sigma) and 10mM Glucose is mixed to the extracted material, lungs and ovaries here, that have been previously hashed with a razor blade. The incubation lasts 1 hour at 37°C under agitation.
2. The suspension obtained is filtered through a 100 µm nylon filter to remove debris.
3. The cells are then pelleted and the supernatant removed. An erythrolysis solution is added for exactly 8 minutes, thereafter, PBS dissolves this solution and the whole is centrifuged.
4. Cells are individualized by passing through a FACS tube lid.
5. The cell isolation can then be processed following the Miltenyi MACS protocol.

Magnetic Beads Cell Sorting - MACS technology

The principle of MACS-Magnetic Cell Sorting is the following: an antibody that is coupled to microbeads is added to the cell suspension and it tags the positive cells. In our case, the microbeads are conjugated to monoclonal rat-antimouse CD11b antibodies. It allows positive selection of mouse monocytes and macrophages.

The positive cells are thus magnetically labeled thanks microbeads. Then, the cell suspension is loaded onto a MACS Column. The latter is placed in the magnetic field created by the MACS Separator. Thus, the magnetically labeled cells are retained on the column while unlabeled cells run through, a fraction depleted in CD11b+ cells, the negative fraction. Finally, to recover only the positive cells, the column is removed from the MACS separator and the remaining cells can be eluted as a positive cell fraction.

4. RESULTS

Preliminary experiments

Co-cultures of tumors cells and macrophages

As a preliminary experiment, co-culture of tumor cells, in this case LLC and B16-F10 cells, and macrophages that are either WT or knock-out for the NALP3 gene was performed.

This experiment was launched to detect and analyze changes in IL-1β gene expression, either at the mRNA or protein level. Because IL-1β is a key mediator of inflammation, we assayed its effect on tumor growth and progression. The premise was that it could provide us with clues about the influence of macrophages on tumor cells and vice versa. Although the addition of LPS and ATP to the medium activates macrophages, signaling cascades could differ according to the genetic background of macrophages. They could also vary as a function of the tumor cell type.

Tumor cells and macrophages were seeded either in the inserts or in the wells as described above. After stimulation by LPS and ATP:

- Supernatants and cell lysates were retrieved for further Western Blot experiments.
- A duplicate set was made to extract the total RNAs from cells.

RT qPCR results

RT qPCR was performed on genes involved in IL-1β processing including IL-1β itself, mIL-1R1 and mNALP3. mβ-actin was used as reference gene. Co-cultures were done in triplicate along with RNA extraction and RT qPCR. Each time, the standard protocol was used, as described above. Expression levels of the different mRNA are shown thereafter.

1. IL-1β expression :

Unexpectedly, the two tumor cell types displayed opposite behavior:

- While an activated microenvironment (WT macrophage) decreased mIL-1β expression in B16-F10 cells, the presence of KO macrophages did not change its expression level, compared to tumor cells cultured alone. This was unexpected since KO macrophages express no active IL-1β.

- LLC put in co-culture express more mIL-1β than cultured alone. Moreover, since IL-1 β induces its own expression, we could expect to see an auto-amplifying loop. However, the co-culture with macrophages (either WT or KO) without any supplemental stimulation also led to an overexpression of IL-1β, showing an active role of the co-culture conditions in the generation of the pro-inflammatory state.

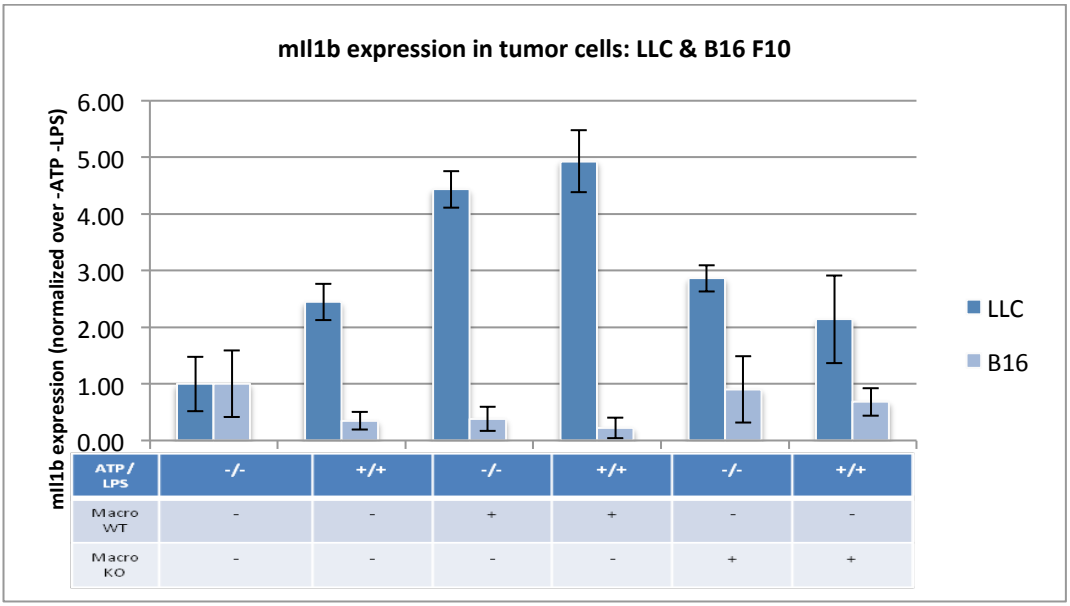

Graph 1: mIL-1β expression level in tumor cells co-cultured with macrophages

The observed difference in response between the two tumor types is intriguing given the importance of IL-1β in a normal microenvironment where it activates the immune response. We could therefore speculate that LLC uses activated microenvironment to further promote activation of the stroma. Contrary, IL-1β present in the microenvironment of B16 F10 tends to diminish their production of this cytokine.

This difference in cytokine production could be one explanation for the two types of cell propagation in the KO background: LLC secrete more IL-1β to better manipulate normal microenvironment and B16-F10 appear to undergo inhibition of IL-1β secretion, a failure that impairs their progression.

However, interpretation of these data has to be done with care since the mRNA level of IL-1β is not representative of the amount of processed and active IL-1β that is secreted by the cells.

Macrophages co-cultured with both tumor cell types increased their basal level of IL-1β expression. Especially for KO macrophages, the expression level remained high since the mRNA is produced but the active form cannot be processed.

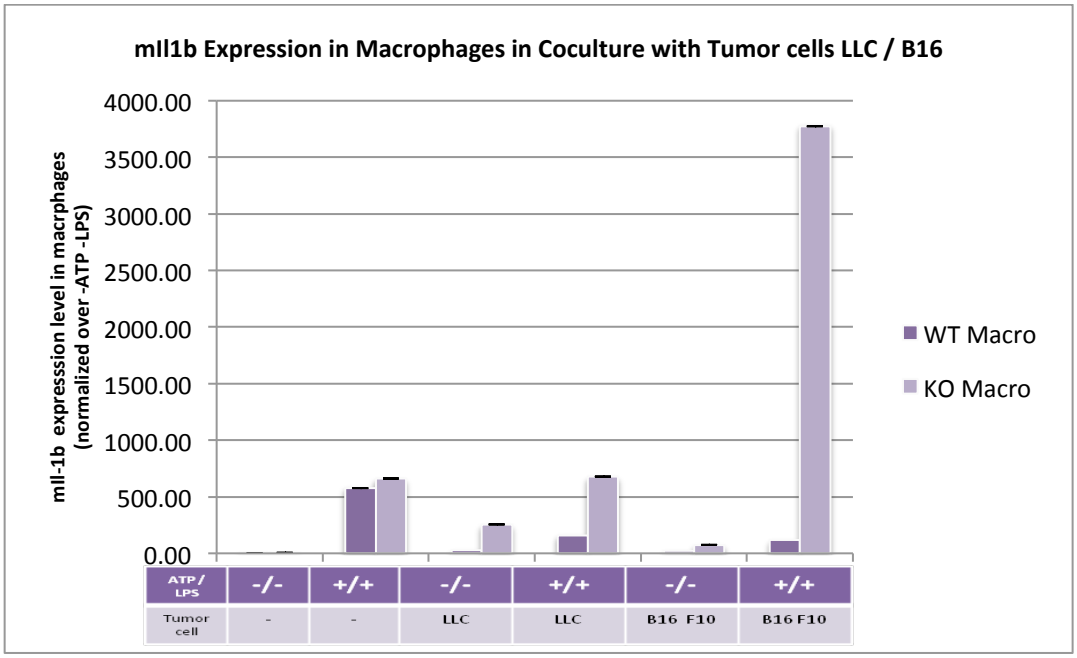

Graph 2: mIL-1β expression level in macrophages either WT or KO, in co-culture with tumor cells

2. Il-1R1 expression:

mIL-1R1 expression level in both tumor types in standard culture is different: B16-F10 mIL-1R1 was detected on the qPCR at the 37th cycle whereas for LLC, mIL-1R1 is already distinguished at the 22nd cycle, representing a 15'000 fold difference.

Secondly, the co-cultures and presence or not of ATP/LPS did not significantly influence the receptor expression level in LLC. For B16-F10, presence of activated macrophages induced more mIL-1R1, an observation that was not made in the presence KO macrophages where the level was comparable to the control case.

Activation of macrophages with ATP/LPS induced up-regulation of the IL-1R1 gene comparably to co-culture conditions. Up-regulation was also lower in KO macrophages. This point seems contradictory since impaired secretion of IL-1β may be expected to induce up-regulation of the receptor to better sense the microenvironment because of the depletion of IL-1β.

In this case, a point worth to investigate is the functional consequences of the difference in receptor expression between the two tumor cell lines. The next step is first of all to detect and quantify this receptor at protein level by the use of a Western Blot. Then, down-and up-regulation of this receptor in tumor cells were performed and described in the next section.

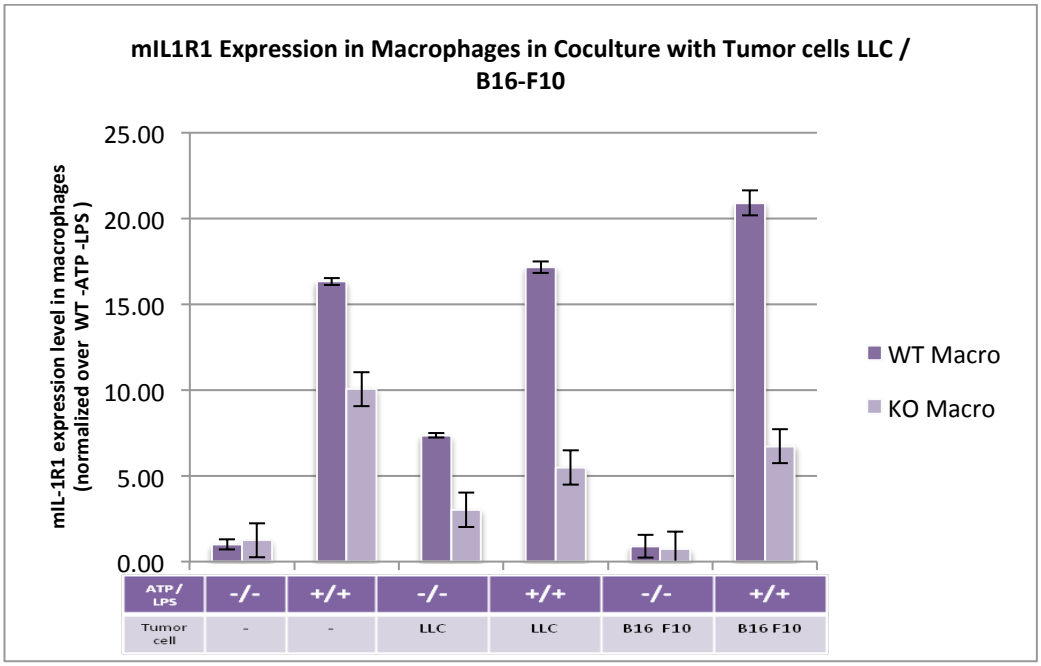

Graph 3: mIL-1R1 expression level in macrophages in co-culture with tumor cells

3. mNALP3 expression:

Presence of macrophages induces the production of mNALP3 in both cell lines where the up-regulation of it is observed. Differences arise depending on the genetic background of the macrophages, either WT or KO, that are in co-culture. This is explained by the fact that immune cells produce a plethora of inflammatory cytokines which may induce various reactions from tumor cells. Up-regulation of NALP3 would allow more IL-1β processing, a notion that is consistent with the observation that more IL-1β is produced by LLC.

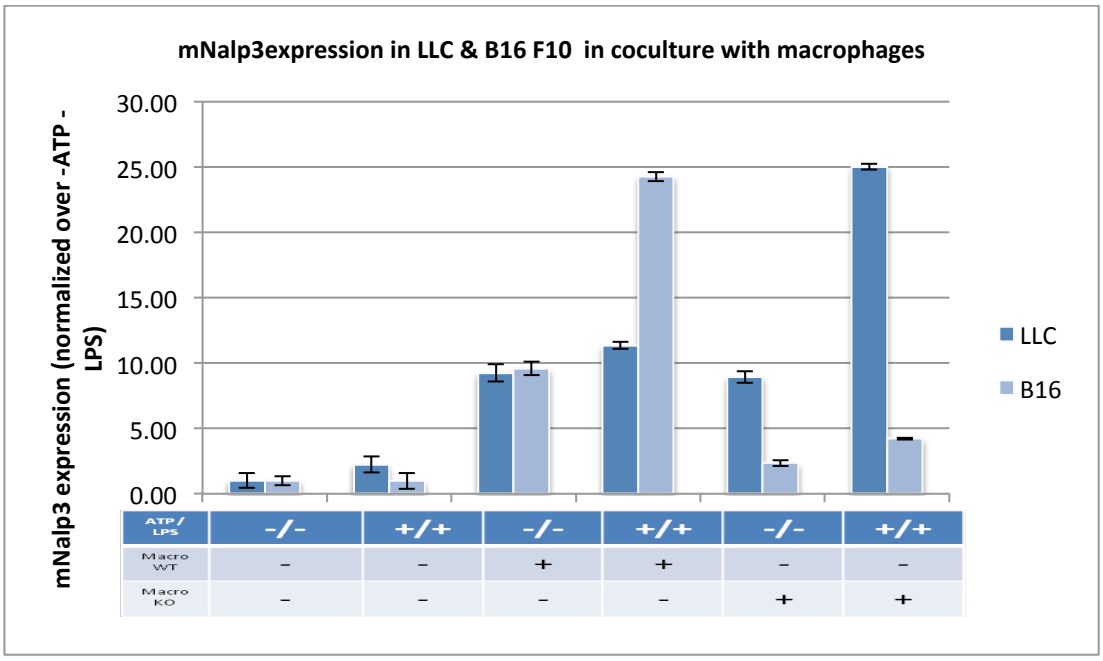

Graph 4: mNALP3 expression in tumor cells in co-culture with macrophages

NALP3 in macrophages subjected to ATP/LPS was up-regulated up to 5 fold. Co-cultures reveal that NALP3 expression is affected by the presence of tumor cells since its expression is decreased in both macrophages as well as in tumor cells.

In conclusion to this experiment, we could analyze the changes induced by co-cultures on three IL-1β related molecules and point out the differences between the two selected cell lines. To better figure out the complex mechanisms regulating these different points, the next step is to broaden the spectrum of genes analyzed by performing microarrays analyses.

RT qPCR on microRNAs

Since microRNAs are also described to be involved in the regulation of immune system, we chose to figure out the expression pattern of some known microRNAs in the macrophages used in our experiments, either WT or KO.

The first experiment allowed analyzing the differences in expression of mir-140-5p in macrophages, with addition or not of LPS and/or ATP. Rnu-5g was taken as reference in this qPCR. Mir-140 was shown in previous studies to be decreased upon addition of IL-1β. Here, LPS and/or ATP treatment of macrophages induces secretion of IL-1β. It will then decrease mir-140 expression.

Practically, we observed that, indeed, the induced IL-1β decreased in the expression of mir-140-5p. LPS also had a stronger effect than ATP in this inhibition. Mir-140-5p expression level in KO macrophages was however higher than in WT macrophages. This can be explained by the fact that these KO cells do not secrete IL-1β as much as WT macrophages do, the inhibition of mir-140 is therefore not as important.

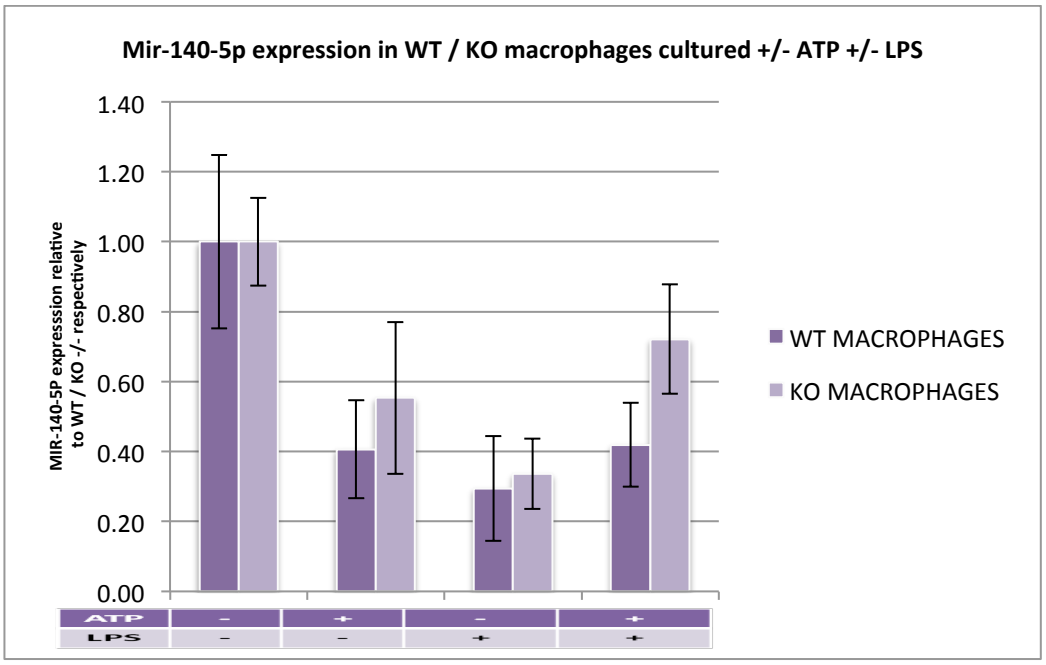

Graph 5: Mir-140 expression in macrophages upon addition or not of ATP and/or LPS

Western Blots

Supernatant and cell lysates were also isolated from co-cultures. The presence of IL-1β was assessed, either in the cell lysate or in the supernatants.

Normalization in this case was made using the Ponceau staining: Photoshop was used to determine whether the pixel intensity for the band at 26kD is the same in each well. IL-1β was detected in supernatant of WT macrophages cultured alone as well as WT macrophages in co-culture with LLC. Note also that without LPS/ATP treatment, this active protein was absent. Moreover, KO macrophages did not secrete the active form. IL-1β proform was detected in the supernatant of co-cultured WT and KO macrophages, revealing that this molecule gets exo-cytosed in the unprocessed form.

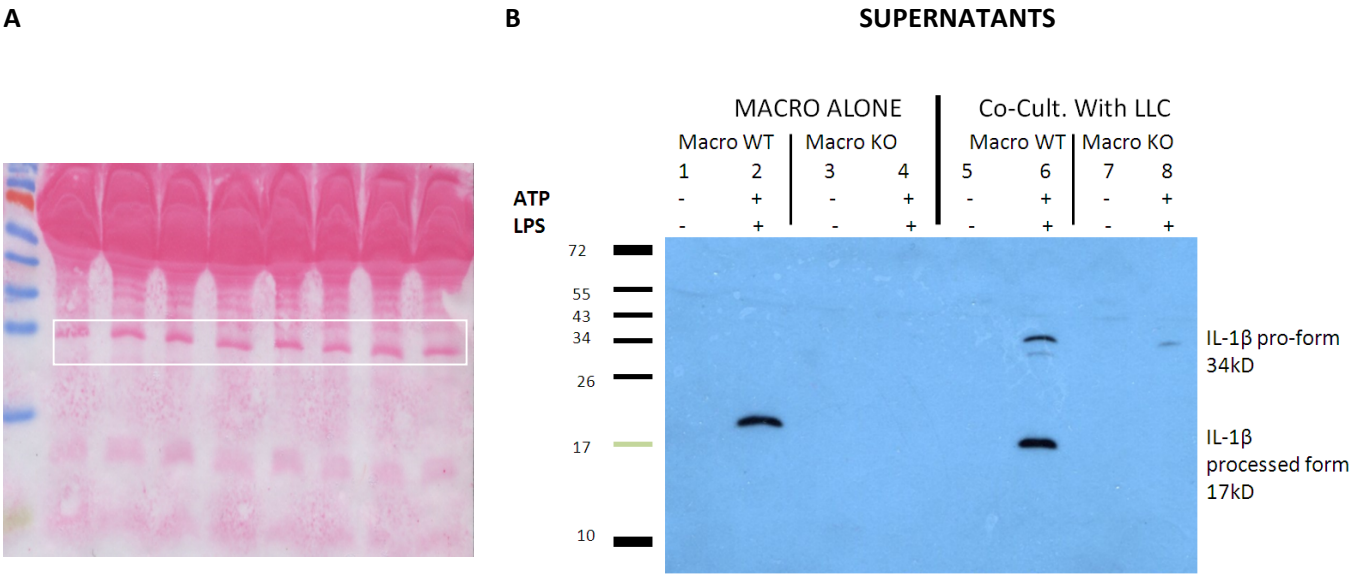

Figure 4.1: A) Ponceau staining realized on membrane representing the supernatant samples, used for normalization of the blot. **B**) WB detecting IL-1β, made on **supernatant of Macrophages** co-cultured with LLC (femto 5 min)

Now regarding cell lysates, western blots were realized to detect IL-1β and IL-1R1. The following table shows the obtained results for the detection of IL-1β:

A

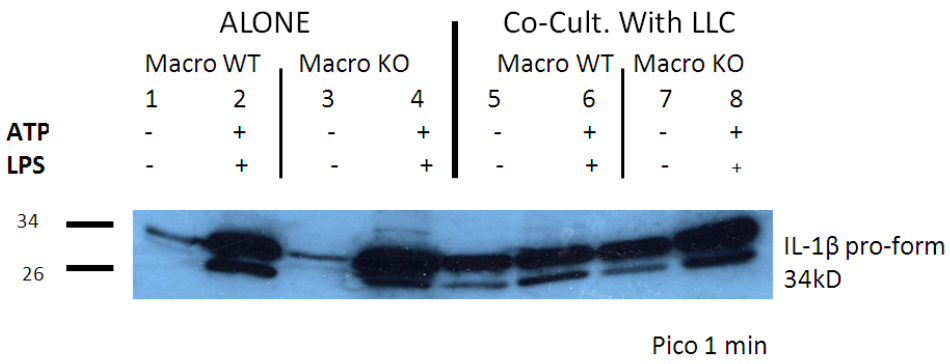

B

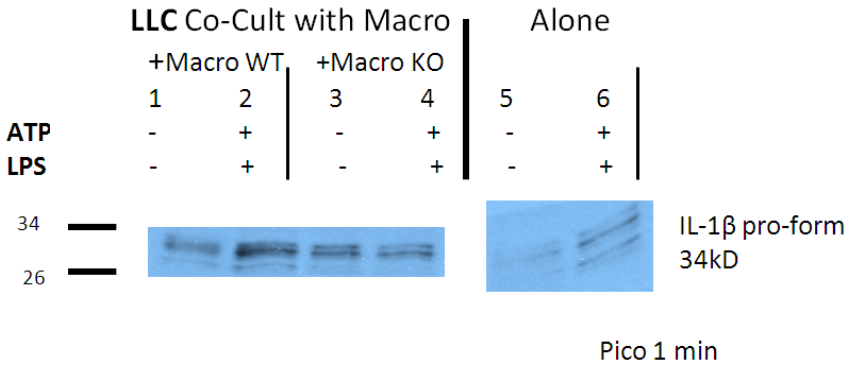

Figure 4.2: A) Cell lysate of macrophages alone or in co-culture with LLC **B**)Cell lysate of LLC alone or in co-culture with macrophages

From Figure 4.2, macrophages alone, either WT or KO, showed high amount of pro-IL-1β, especially upon addition of LPS/ATP. In co-cultures too, the pro-form was detected, especially in KO macrophages in presence of LPS/ATP. An accumulation of this protein happened here, probably because it cannot be processed.

On the side of LLC, the co-culture strengthened the expression of the pro-form of IL-1β. To test the influence of LPS/ATP on them, we also cultured these cells alone with or without these chemicals. We could see a slight activation of the gene since more pro-form was detected upon their addition.

The western performed to detect IL-1R1 in cell lysates was too noisy to perceive the right 80kD band. The IL-1R1 anti-body used was subjected to different dilution tests to optimize its use.

IL-1R1 : silencing and overexpression

As explained in the previous paragraph, the observed difference in IL-1R1 in the two cell lines especially aroused our curiosity: could this receptor be implicated in the metastatic capacity of either of these two different cell types?

To answer this question, the first thing we did was to either silence or overexpress this receptor in tumor cells. The silencing was designed using a small hairpin (sh) and induced in the two selected tumor cell lines. Then, the overexpression procedure was realized. The correct silencing and overexpression of the gene were then tested using standard RT qPCR protocols.

Here followings are the results of the qPCR made on both B16-F10 and LLC tumor cells transformed with:

- sh762 representing the most efficient silencer of IL-1R1
- sh916 is a less efficient silencer for the same mRNA
- shCTL represents the negative control.
- OVER sample stands for the cells that were infected with the virus containing the overexpression construct.

RT-qPCR

1. mIL-1R1 expression level

We can see a difference in efficacy of the down-regulation in the two types of cells: B16 F10 clearly showed lower expression of mIL-1R1 than LLC, indicating a more efficient down-regulation in them. This could arise from different in virus penetration of the cells. Nevertheless, since LLC express mIL-1R1 15'000 fold more than B16 F10, the sh could work and decrease the expression level to a value that is still high enough and thus, the down-regulation is unnoticeable.

This difference in efficacy was also observed for the overexpression. It worked very well in B16 F10 cells whereas in LLC, only 4.27 fold more are detected.

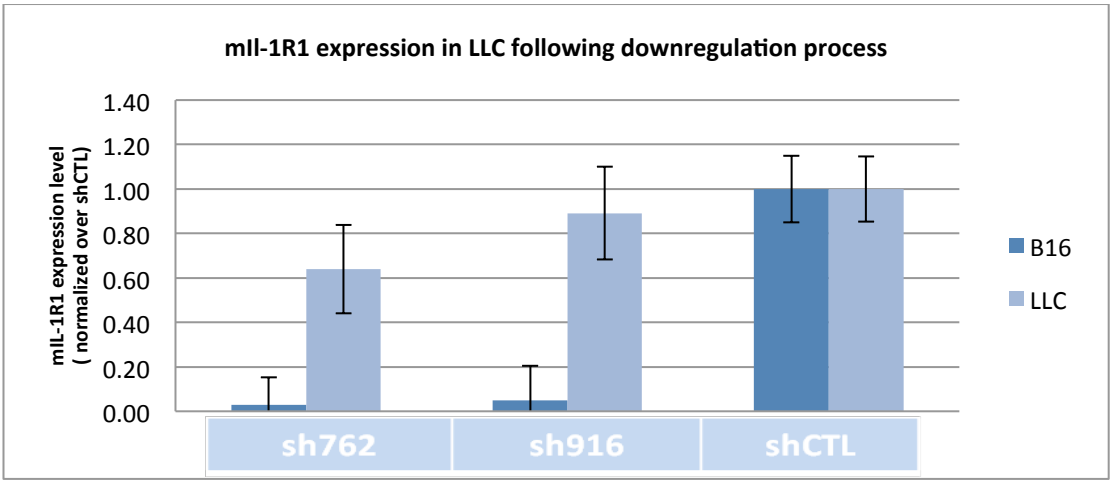

Graph 6: mIL-1R1 expression level in B16-F10 and LLC cells, upon downregulation of the receptor

Tumor cell type	sh CTL	OVER-expression
B16-F10	1.00	2144.60
LLC	1.00	4.27

Table 2: mIL-1R1 expression level in tumor cells, upon overexpression of the receptor

2. mIL-1β expression level

With the most efficient sh, the sh762, mIL-1β expression level was higher than in the control, as well as in the overexpressed case. This was true for both cell lines.

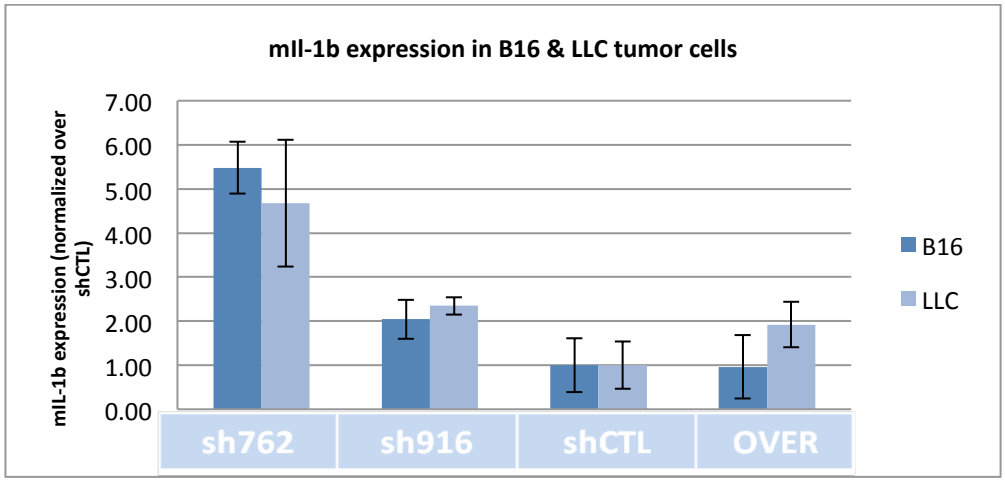

Graph 7: mIL-1β expression level in B16-F10 and LLC cells, with up- or downregulation of the receptor

3. mIL-18 expression level

This cytokine is a target gene of IL-1 signaling and its own signaling cascade shares different intermediate mediators. Here what was observed was that mIL-18 was upregulated in both down- or up-regulation of the receptor IL-1R1.

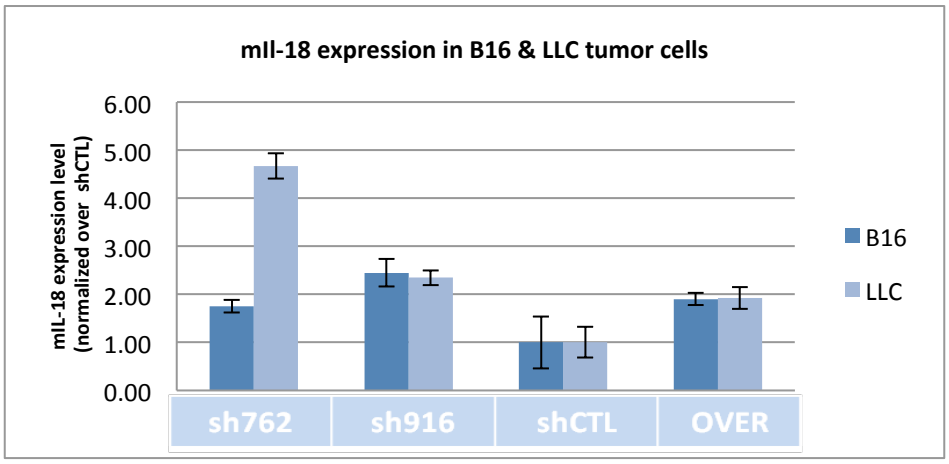

Graph 8: mIL-18 expression level in B16-F10 and LLC cells, upon downregulation of the receptor

Shared intermediates in the signaling pathway such as MyD88 or IRAK were not analyzed but we reckon that every step could stand for the rate limiting point of the cascade and would thus require deeper investigations upon these specific genetic modifications.

Western blot

After having analyzed the mRNA levels, the next step was to check the effect of the modifications on protein level. The results of the western blot performed on B16 F10 cell lysate to detect IL-1R1 are presented in figure 4.3:

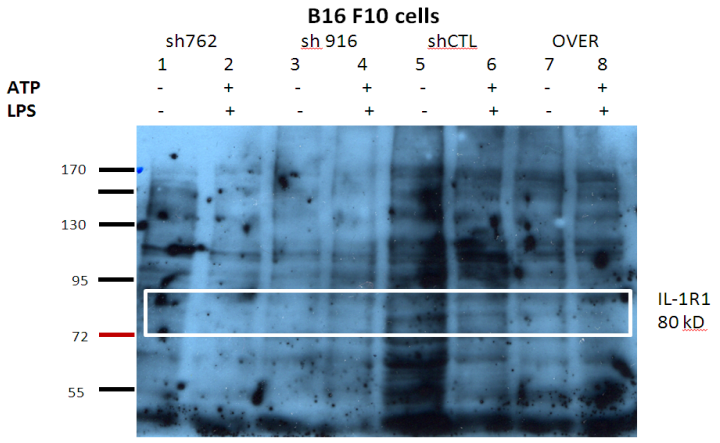

Figure 4.3: IL-1R1 western blot detection on B16 F10 cell lysate

As we can see, this western blot showed a lot of background noise that could arise for different reasons:

- × The blocking with milk was not sufficient in terms of time: a longer blocking step could improve the efficiency of the primary antibody
- × The incubation with primary anti-body at 4°C instead of room temperature would be more efficient, since high temperature increases the risk of off-target recognitions.
- × It can also be the result of a secondary antibody that recognizes different non-specific targets.

Proliferation Assay

When a genetic modification is introduced in a cell line, the potential changes induced at the proliferative levels have also to be checked.

The results of the proliferation assay are presented in the graph 9 in which the principle is: the higher the measured absorbance, the higher the proliferation rate. No significant differences in proliferation were observed. In B16-F10, the downregulation of the receptor provoked a slight decrease in proliferation. Since the absorbance is proportional to the formazan quantity released from cell, it mainly depends on the physiological state of the cells, a factor that can differ in cells having undergone specific rounds of selection.

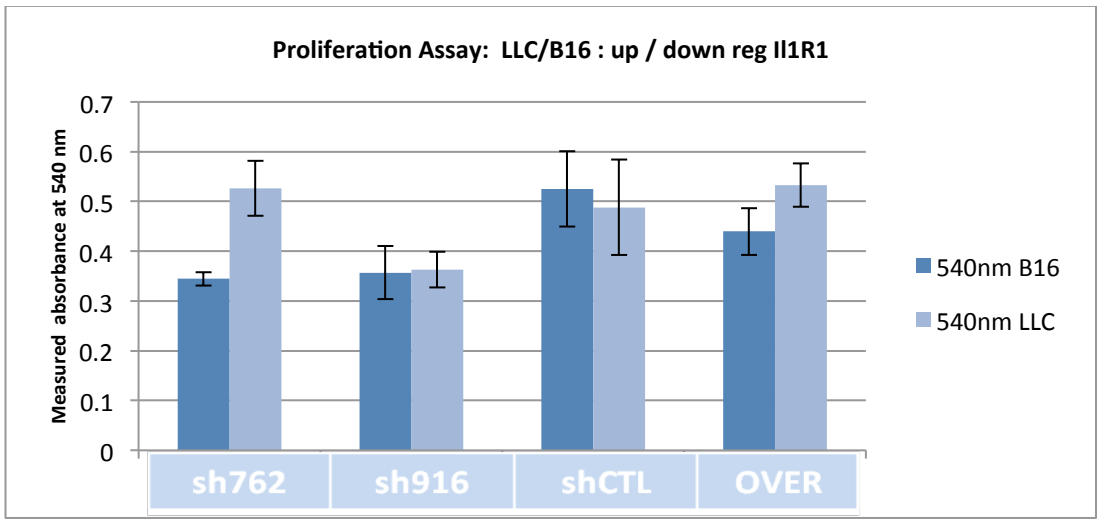

Graph 9: Proliferation assay made tumor cells, with over or down-regulation of the IL-1R1 receptor

Migration Assay

A migration assay was also performed to check the ability of modified cells to migrate and thus to heal wounds. Here following is the analysis process of the different pictures taken during the experiment to follow the migration of both cell types. This was made using different ImageJ manipulations as described in Figure 4.4.A).

Since B16 F10 have a completely different morphology compared to the round LLC, it was choose not to count them but to define the percentage of the scar zone that was occupied by the cells at every time point(see Figure 4.4.4).

A

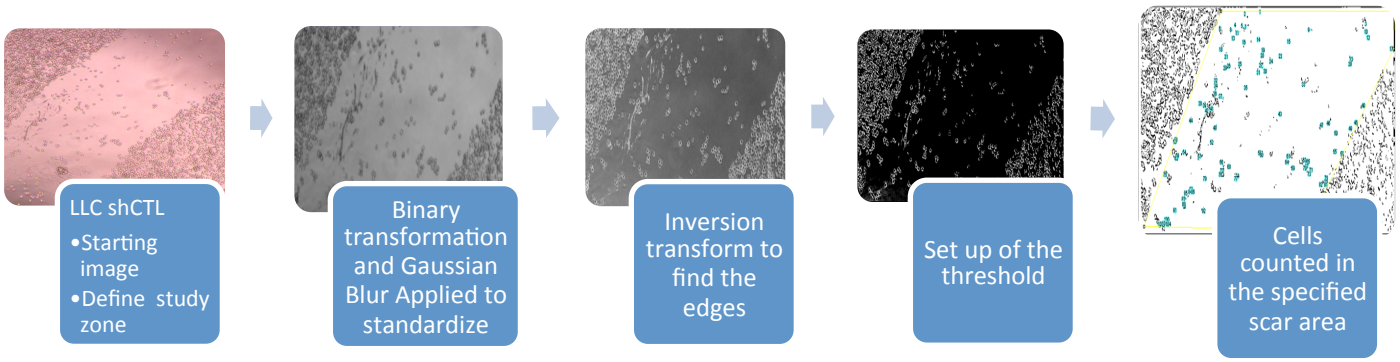

1. B16 F10 sh762 at timepoint **0h**

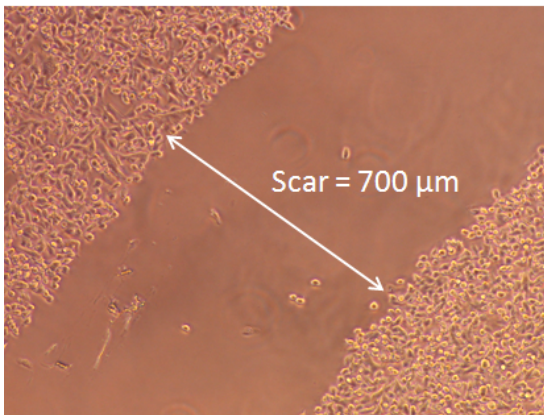

2. B16 F10 sh 762 at timepoint **24h**

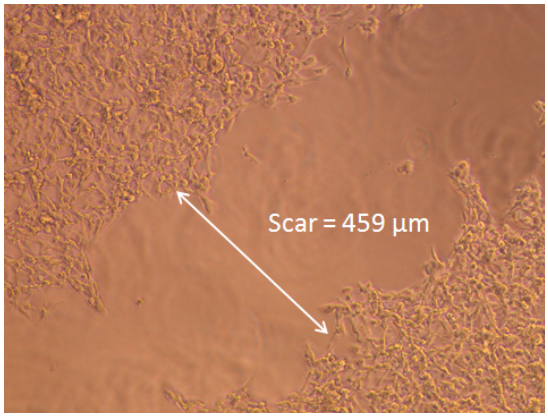

B16 F10 at timepoint **48h**

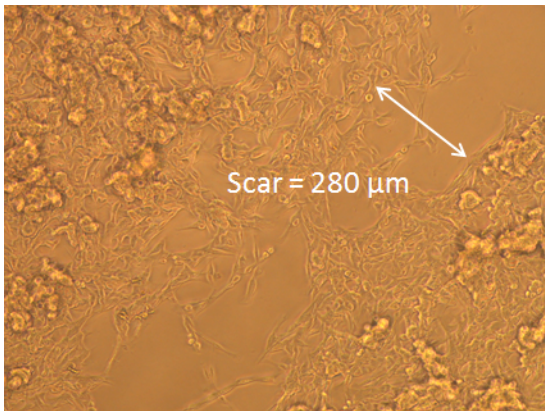

3. Determination of the surface occupancy by B16 F10 cells (made for each condition)

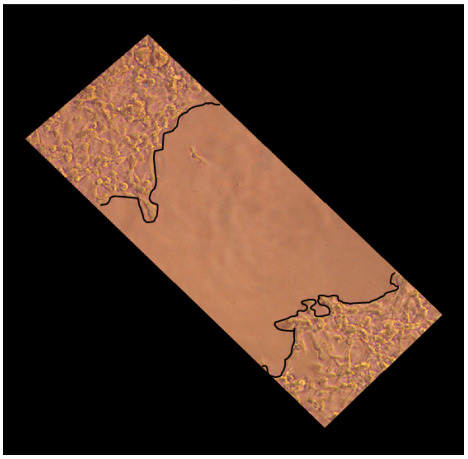

Figure 4.4: A) Image J processing method for the LLC pictures **B)** Images of the scar evolution with time in the case of B16 F10 sh762 cells : **1-** at oh , **2-** at t=24h , **3-** at t=48h , **4**- image representing the way of analyzing the surface of the scar the migrating cells do cover

Two measures were computed: either the scar size with time or the percentage of the scar area that was re-occupied with cells.

In the case of LLC, the number of cells present in the scar zone was counted and then, approximating the size of a round LLC cell, the surface area could be determined. For the B16 F10 cells, the percentage of scar re-occupation could be computed by determining the zone of the scar occupied by cells (Figure 4.4.4). The obtained graphs are shown below.

Migration was not impaired by any of the three genetic modifications in B16 F10 cells, as it can be seen in graph 10. However, the migratory rate was not equal for all the conditions.

Graph 11.A) shows the percentage of scar area that was covered by tumor cells with time: B16 F10 sh762 cells did migrate more quickly at the beginning: after 24 hours, double quantity of cells was already investigating the scar. However, at 48 hours, every cell type showed similar scar occupancy. The pictures were taken in this case every 24 hours. To better follow the migration process, it could have been more instructive to have taken pictures every 6 hours.

Scar size was decreasing linearly with time especially for the OVER case. It reflects the stronger ability of B16 F10 OVER to investigate the scar more widely in the end. This last point could also be explained by the increased proliferation of these cells.

A

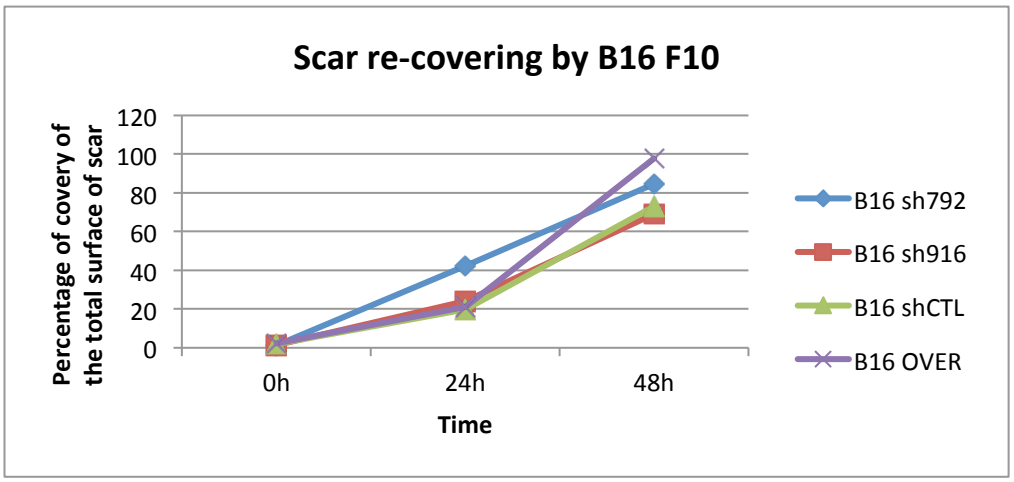

B

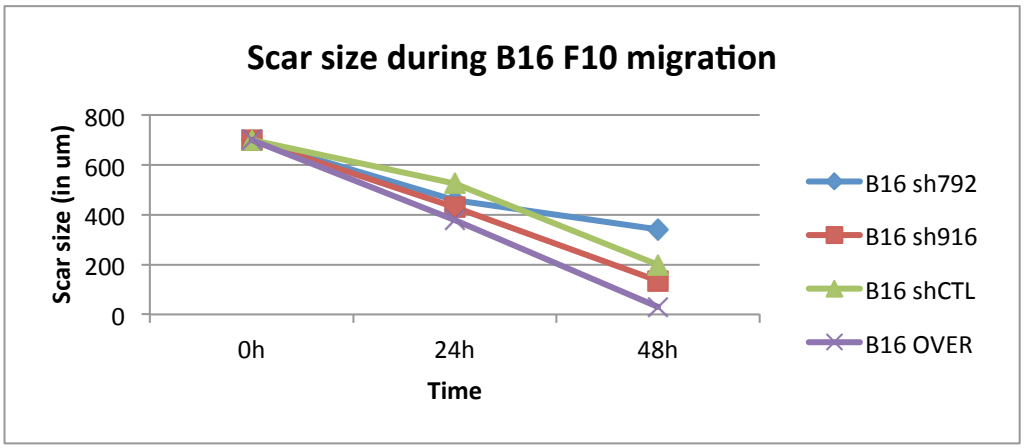

Graph 10: A) Migratory scale of B16 F10 cells from scar timepoint till total confluence of cells. **B**) Size of the scar for the different conditions during the time of the assay.

For the LLC, since these cells are semi-adherent, we would have expected that they would not be able to migrate with a directional movement. In fact, these cells were also migrating as it can be seen in figure 11, with LLC sh762 being the quicker ones since after 48 hours, a state of confluence was achieved. In this case, the downregulation of the receptor did not seem to have increased the migratory rate: the LLC OVER only recovered half scar zone after 48 hours. Regarding the scar size, we can see that it decreased more rapidly in the case of LLC sh762.

A

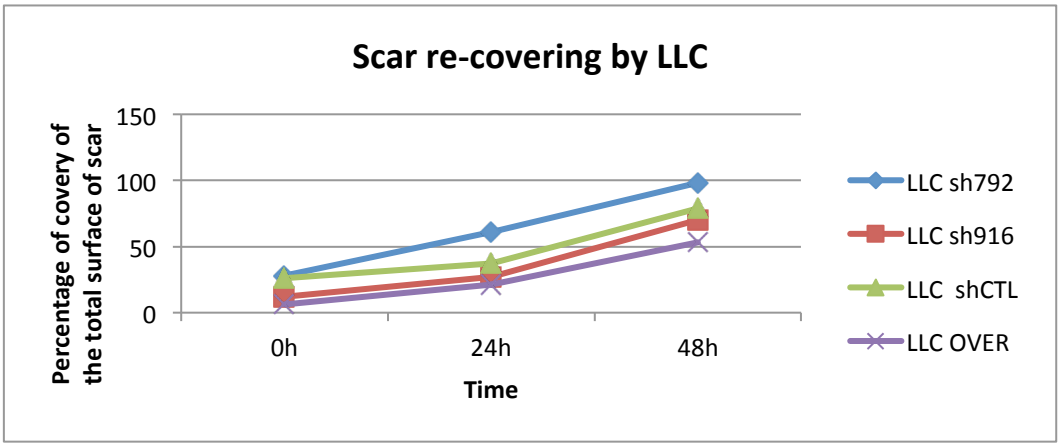

B

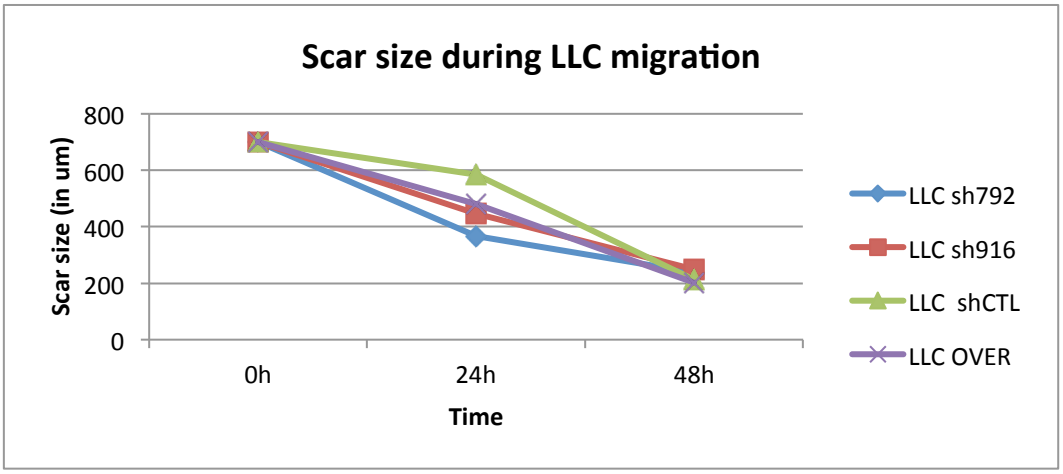

Graph 11: A) Migratory scale of LLC cells from scar timepoint till total confluence of cells. **B**) Size of the scar for the different conditions during the time of the assay.

To conclude this experiment, we can say that the induced genetic modifications did not influence the migration capacity. However, these assays were performed under normal conditions, with standard medium. To better assess the importance of the receptor up- or down-regulation, the use an IL-1β neutralizing antibody would block the signaling through the receptor and therefore, we could investigate the effects of this inhibition and determine if IL-1R1 is a rate limiting component.

Soft Agar Assay for colony formation

This assay tests the anchorage independent growth of cells. Moreover, the apparition of colonies in soft agar often indicates *in vivo* carcinogenesis capacity.

Concerning the B16-F10 cell, we tested all 4 constructions, i.e. sh762, sh916, shCTL and OVER. Colonies began to appear at day 7-8 and were significant at day 11-13. The morphology of the colonies was similar, with a round-shaped form in all cases but at D13, some sh762 colonies already began to spread in a star fashion. Considering the size of the colonies, it could be measured using pictures with a same magnification. At D11, the sh762 presented the bigger colonies: 1,8 fold bigger than shCTL. In this particular case, we could observe more but smaller colonies.

However, except these differences in morphology and size, we could not distinguish significant differences in the establishment of these colonies, indicating that the induced modifications are not impairing the anchorage independency for B16 F10 cells.

Concerning the LLC, we could count the number of colonies (under a given field of view, at a magnification of 40X) and we got the following numbers:

	LLC sh762	**LLC shCTL**	**LLC OVER**
Number of colonies	5 (± 2)	6(± 2)	11(±2)

Table 3: Number of colonies count for LLC cells in the soft agar assay

A higher number of colonies was counted in the case of overexpression compared to downregulation. Regarding their morphology, all colonies were similar in shape with a round form.

The main conclusion for these *in vitro* assays is that the global phenotype regarding proliferation, migration and anchorage independent growth is conserved and not affected by the induced genetic modifications. As preliminary tests, these were performed under standard conditions, with normal medium and without other stimulation or perturbation. Then, different more sophisticated tests would allow better understanding IL-1R1 importance in these tumor cells:

- change the medium composition by complete depletion of IL-1β by the use of a neutralizing anti-body
- culture the cells with different concentrations of IL-1β
- culture the cells with macrophage (WT or KO) culture medium

- check downstream mediators expression levels (mRNA and protein), especially NF-κB.

***In vivo* experiments**

After *in vitro* tests, the investigations at the *in vivo* level were done. Such *in vivo* tests are more relevant and accurate to figure out real impact of genetic modifications, since every player is represented, with complete microenvironment. To do so, we decided to perform two assays, with each time, sh762, shCTL and overexpression, in B16-F10 and LLC:

- Sub-cutaneous injections (500'000 cells in each condition) were made to assess the primary tumor growth capacity of the modified cells.
- Tail-vein injections (500'000 cells in each condition) allowed assessing the metastatic spread, with cells introduced directly into the circulation, bypassing the need of primary tumor.

14 days after injections, the mice were sacrificed and the subcutaneous tumors were retrieved, as wells as the lungs and livers for the tail-vein injected mice.

Concerning the sub-cutaneous tumors, the primary observations were that the downregulation of the receptor did not impair *in vivo* growth since the size of the tumors was smaller than the control case but still present and this, for both tumor cell types. Subcutaneous tumor volume could be calculated using the ellipsoid volume formula, postulated by Reynolds and Tomayko to be more accurate than the spherical volume to determine real volume of subcutaneous tumors [42]. The ellipsoid formula is as following: $V = \left(\frac{\pi}{6}\right) * L * W * H$ We used it to determine the volume of subcutaneous tumors.

	SC tumor volume (mm^3)		SC tumor volume (mm^3)
B16 F10 sh762	**52** mm^3 (±5 mm^3)	**LLC sh762**	**340** mm^3 (±5 mm^3)
B16 F10 shCTL	**290** mm^3 (±5 mm^3)	**LLC shCTL**	**430** mm^3 (±5 mm^3)
B16 F10 OVER	**41** mm^3 (±5 mm^3)	**LLC OVER**	**0** mm^3 (±5 mm^3)

We could observe a difference in tumor size for the sh762 versus the shCTL, confirming that downregulation could play a role in decreasing growth capacity of the given cells. The overexpression showed intriguing results: there was only a very small tumor in the case of B16-F10 cells and even no tumor at all present for the LLC. This was a bit surprising, since we expected to improve tumor growth with increased receptor representation at the cell surface.

The extracted organs were sent for paraffin inclusion and hematoxylin-eosin coloration. These subcutaneous tumors were mainly composed of cancer cells with a high percentage of necrotic tissues. The immune cells infiltrate was present but it was difficult to qualitatively quantify it.

In the case of tail-vein injected mice, the extracted tissues, lungs, livers and ovaries, were fixed in paraformaldehyde before to be included in paraffin for hematoxylin-eosin coloration. We

could then count the number of metastases in every sample. Lungs did not present many metastases compared to livers, this is why we chose to evaluate more deeply liver colonization.

	B16 F10 sh762	B16 F10 shCTL	B16 F10 OVER
Number of Metastases	2 (±1)	4(± 1)	3(±2)
	LLC sh762	**LLC shCTL**	**LLC OVER**
Number of Metastases	4 (± 2)	5(± 2)	9(±2)

Table 4: Number of metastases count for B16 F10 and LLC TVI in livers extracted

In the case of LLC, the metastases were globally small and widely dispersed all around the liver. LLC overexpression presented more metastases, even if these were very small. LLC sh762 also showed small metastases, but less than with shCTL. Moreover, infiltrates were present, mainly next to blood vessels.

For B16, we could observe bigger metastases but in lower number. sh762 B16 F10 presented metastases but these were smaller in size compared to shCTL. Necrotic tissue was present in metastases of all three conditions, indicating a state of the metastases that is more advanced than in the case of LLC. Infiltrates were also detected mainly beside blood vessel.

IN VIVO studies

Metastases gene expression profiling

After having performed co-cultures mimicking the inflammatory micro-environment, we decided to figure out the gene expression profile of B16-F10 metastases in both NALP3 WT and KO background in an *in vivo* experiment. To do so, we tail-vein injected 500'000 B16-F10 cells in 5 WT and 5 KO C57Bl/6 mice. These tumor cells were normal concerning IL-1R1 expression but they expressed luciferase to follow the establishment of metastases with Xenogen. Sacrifice of WT and KO mice was not done at the same time since melanoma cells establish metastases more easily into the WT background. WT mice were thus sacrificed at day 19 and KO at day 22. The extraction of the organs, lungs and livers, was realized following a specific protocol to avoid RNA degradation, being directly snap-freezed. Thereafter, LCM protocol was lauched with preparation of slices for every sample followed by staining, dehydration, Laser Capture Microdissection and total RNA extraction.

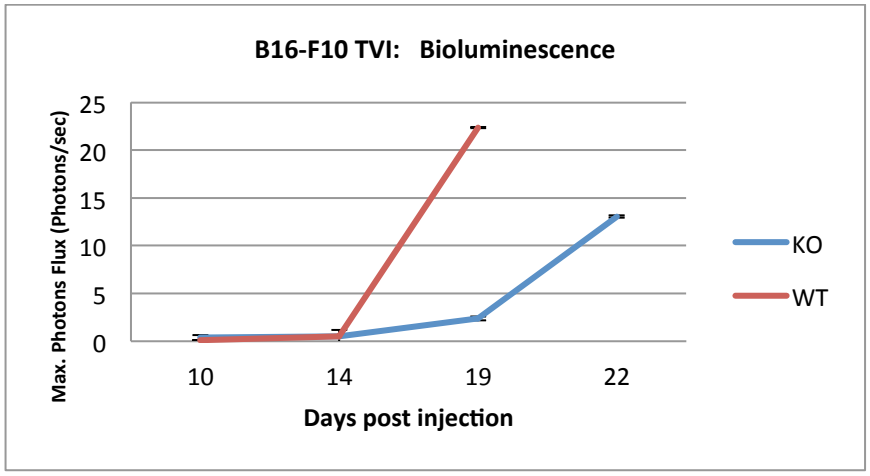

Graph 12: Bioluminescent signal obtained of B16-F10 metastases in C57Bl/6 mice

Macrophages in contact with metastases gene expression profiling

Since it is more relevant to isolate specifically macrophages that are in contact with metastases than cutting stromal area containing a mix of immune cells by laser capture, we set up another experiment: tail-vein injection of B16-F10 cells (500'000 cells) in both WT and KO female mice, sacrifice after 21 days, extraction of organs followed by specific isolation of macrophages.

In this experiment, organs retrieved were the lungs and the ovaries: B16-F10 metastatic spread shows organ-specificity in a nonrandom distribution. In female mice, most metastatic niches are found in lungs and ovaries. Since in this case, the goal was to isolate macrophages in contact with established metastases, we indeed took the lungs and ovaries.

Morphologically, the extracted WT lungs showed only two apparent metastases, the KO one did not present any. In ovaries, it was striking to see the difference between WT and KO mice: WT ovaries were around 10 fold bigger than normal ovaries and KO ones were bigger as well, but to a lesser extend.

The extracted organs were prepared as explained in the methods part to specifically isolate macrophages. A FACS analysis made on pre- and post-sorted populations allowed saying that the isolation was efficient:

- In lungs, the population of $CD45^+$cells, corresponding to immune cells, was more important: permissiveness of this organ is higher since metastases are more widely dispersed all around the organ, so that infiltration by immune cells is easier. Moreover, population of $CD11^+$ cells in the negative fraction after sorting was around 4% of immune cells and the positive fraction of 90%.
- In ovaries, we could expect infiltration to be more difficult for immune cells: detected $CD45^+$ cells were less represented than in lungs. The $CD11^+$cells population was indeed lower, with only 3.15% of total immune cells detected by FACS. In the negative fraction, only 0.04% of $CD11^+$cells were detected, while in the positive one, 8,7 % of cells were positive.

Interestingly, only 57% of lung cells were $CD45^+$ (common leukocyte antigen) in the NALP3 KO mouse, versus 78% for the WT lung: the lack of IL-1β secretion in NALP3 KO mice leads to a lower accumulation of immune cells upon B16-F10 metastases stimulation.

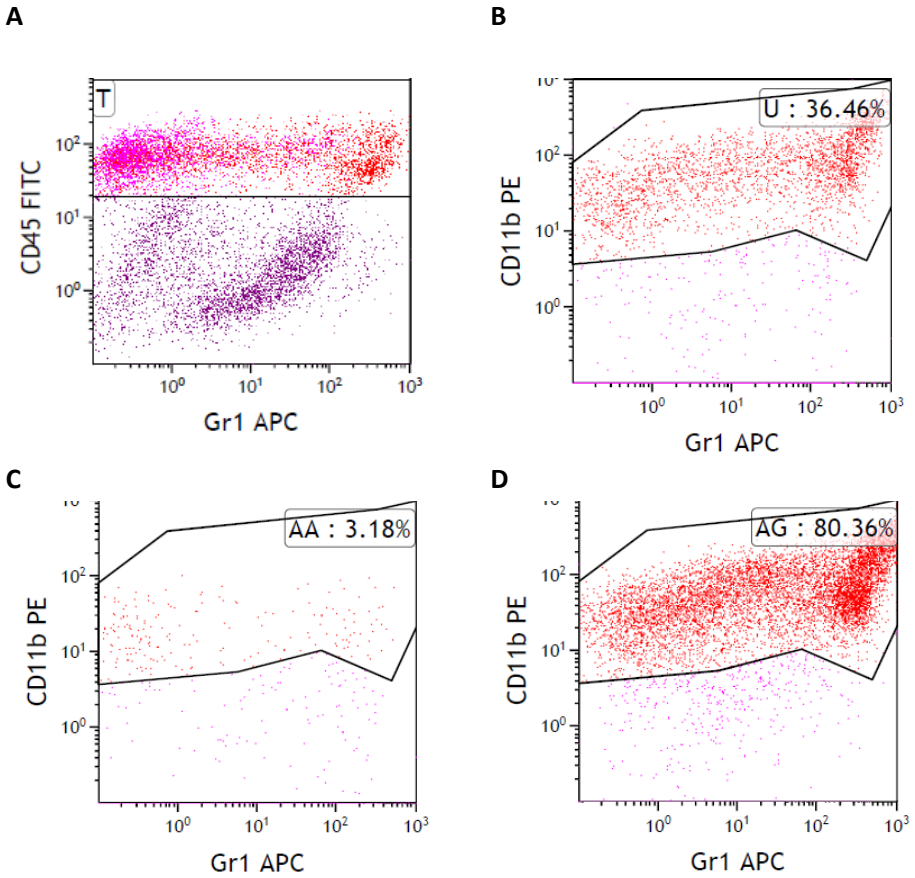

Graph 13 : FACS analyses of **A**) sorted immune cells (red and pink) in lungs **B**) sorted monocytes (red) in lungs **C**) monocyte population in the negative fraction of lungs (red) **D)** monocyte population in the positive fraction

After isolation of macrophage population, we extracted totRNA from these samples as described before. This material was then sent to the DAFL for further micro-arrays gene expression analyses. The goal is to figure out the differences in gene expression profiles between WT and KO macrophages being in physical contact with tumor cells, at metastatic niches.

5. DISSCUTION & PERSPECTIVES

The present study tried to figure out significant aspects of metastatic spread regarding two different cell lines with paradoxical behavior. The NALP3 mouse model helped us assessing the importance of the IL-1β cascade in the promotion of metastases by playing with inflammatory context. Collected results pointed out that genetic and epigenetic modifications are exploited by cancer cells for their malignant evolution and spread. Moreover, we noticed opportunistic adaptation to host physiology, resulting in different patterns of gene expression profiles.

First of all, the simulation of cancer microenvironment we could re-create by the use of inserts was conclusive to demonstrate influence and cross-talk that take place between tumor cells and macrophages. Regarding tumor cells, this experiment was also helpful in distinguishing the opposite behavior the two selected cell lines. LLC, more independent of immune activation, secretes a lot of cytokines, playing themselves the role of activating cell. These cells moreover express a basal level of mIL-1R1 that is high compared to B16-F10, another point that could account for their independency. On the other hand, B16-F10 cells are more dependent on an activated microenvironment: their cytokine secretion is decreased upon contact with immune cells in the experiment. The two opposite behavior observed are render investigations more relevant in the context of NALP3, since the latter plays an important role in the release of IL-1β in microenvironment.

Gene expression analyses for macrophages of different NALP3 background were instructive in terms of adaptation mechanisms: cross-talks with tumor cells induced more receptor to be expressed, with a concomitant up-regulation of the NALP3 gene itself. These facts reflect the influence tumor cells can induce in their microenvironment, rendering the latter a major contributor of metastatic progression. The protein level analyses confirmed these influences.

These preliminary experiments led us to consider gene expression studies with a plethora of different gene. To calk real metastatic events, we performed *in vivo* experiments by the injection of cells in both NALP3 backgrounds. Laser microdissection allowed specific metastatic niches isolation and the extracted samples allowed performing micro-arrays to figure out the gene expression profiles of B16-F10 metastasizing in both backgrounds. The results that will come out from this experiments will certainly highlight different signaling cascades that are involved, opening new insights to further investigate this mouse model and its relevance.

Concerning the study of microenvironment gene expression, we decided not to use laser assisted microdissection, since different cells would be extracted in that way. The extraction of fresh macrophages upon injection of B16-F10 was therefore performed, using organs strongly invaded by tumor cells. We expect these macrophages to be associated and in direct contact with metastatic niches. The next step of this experiment that is now set up will be to launch microarrays in order to figure out adaptation mechanisms involved.

Knowing gene expression profiles from both sides will be more instructive, allowing better appreciating and understanding of occurring crosstalk, especially at the level of cytokines and chemokines secretion pathways.

The basic investigations at the level of IL-1R1 were also preliminary: we could demonstrate that modification , either up- or down-regulations, did not change global phenotypical traits such as proliferative and migratory capacities. However, as explained before, it was standard and preliminary *in vitro* tests to perform before investigating in more details the role of this key immune receptor.

The *in vivo* experiments figured out that overexpression of this receptor did not induce a stronger metastatic spread of tumor cells. We could explain that by the fact that this receptor, beside its implication and importance in immune cells, shares many downstream signaling molecules with a myriad of other key signaling cascades. The next steps here would be to investigate this complex signaling pathway and try to figure out which one represents the real limiting factor. Since IL-1β cascade mainly signals through NF-κB, we also want to investigate more deeply at this level. Moreover, NF-κB signaling could influence NALP3 background in several ways that are not described yet. However, the work on IL-1R1 to diminish propagation of tumor cells could represent a real and targetable appealing new key molecule, at least for a given set of tumor cells.

These exciting new insights will hopefully be further investigated in the next months. We reckon that the NALP3 mouse model will be very instructive to figure out complex events of metastatic spread, in which so many proteins choreograph with different molecular patterns.

6. REFERENCES

1. Ferlay, J., *et al*., *Estimates of cancer incidence and mortality in Europe in 2008*, European Journal of Cancer, 2010, 46, p.765-781.
2. Hanahan, D. and R.A. Weinberg, *The hallmarks of cancer,* Cell, 2000, 100, p.57-57
3. Mauch, C. *et al, Tumor-stroma interactions: their role in the control of tumor cell invasion and metastasis,* JDDG, 2006, 4, 496-502
4. Mantovani, A., *Preface,* Cancer Metasatsis Review, 2010, 29:241
5. Albini, A., *et al.* , *The tumour microenvironment as a target for Chemoprevention*, Nature Reviews Cancer, 2007, 7, p. 139-147.
6. Mueller, M. and N. Fusenig, *Friends or foes, bipolar effects of the tumor stroma in cancer*, Nat Rev Cancer, 2004, 4, p.839-849
7. Joyce, J.A, *Tumor-host interactions: implications for developing anti-cancer therapies,* Expert Rev Mol Med, 2006, 8, p.1-32
8. Whiteside, T. *et al* , *The tumor microenvironment and its role in promoting tumor growth,* Oncogene, 2008, 27, 5904-5012
9. Coussens, L. and Werb Z., *Inflammation and cancer,* Nature, 2002, 420, p.19-26
10. Ruegg, C. *et al, The tumor microenvironment and its contribution to tumor evolution toward metastasis*, Biochemistry and cell biology , 2008, 6, p.1091-1103
11. Mantovani, A. *et al, Cancer related inflammation,* Nature Review, 2008, 454, p. 436-444
12. Balkwill F, Mantovani A. , *Inflammation and cancer: back to Virchow?,* Lancet, 2001;357, p. 539-45
13. Porta, C., *Tumor promotion by tumor-associated macrophages,* Adv Exp Med Biol. 2007, 604, p.67-86
14. Karin, M., *NF-κB and STAT3 - key players in liver inflammation and cancer*, Cell Res. 2011, 21, p. 159-68
15. Karin, M. *et al*, *Immunity, inflammation, and cancer*. Cell, 2010, 140, p. 883-99
16. Hornung, V., *Inflammasomes: current understanding and open questions*, Cell Mol Life Sci, 2010, 68, p. 765-783
17. So, A., *et al, Regulation of inflammasome activity*, Immunology Reviews, 130, p. 329-336
18. Kubista, M, *et al, The real-time polymerase chain reaction* Mol Aspects Med. 2006,27, p. 95-125
19. Petrilli, V., Papin S, Tschopp J, The inflammasome, Curr. Biol., 2005, **15**:R581.
20. Andrei, C. *et al., Phospholipases C and A2 control lysosome-mediated IL-1 beta secretion: Implications for inflammatory processes.* , Proc. Natl. Acad. Sci, 2004, 101: 9745-5
21. Gattorno, M. *et al., Pattern of interleukin-1beta secretion in response to lipopolysaccharide and ATP before and after interleukin-1 blockade in patients with CIAS1 mutation*, Arthritis Rheum. 2007, **56**, p.3138-48

22. Apte, R. , Voronov, E., *Interleukin-1: a major pleiotropic cytokine in tumor-host interactions,* Cancer biology, 2002, 12, p.277-290

23. Castelli, C. *et al*, *Expression of interleukin 1 alpha, interleukin 6, and tumor necrosis factor alpha genes in human melanoma clones is associated with that of mutated N-RAS oncogene,* Cancer Res. 1994, 54, p. 4785-90.

24. Beaupre, DM. *et al*, *Autocrine interleukin-1beta production in leukemia: evidence for the involvement of mutated RAS,* Cancer Res. 1999, 59, p.2971-80.

25. Vidal-Vanaclocha, F. *et al, Interleukin-1 receptor blockade reduces the number and size of murine B16 melanoma hepatic metastases* , Cancer Res. ,1994, 54, p.2667-72.

26. Vidal-Vanaclocha, F. *et al , Interleukin 1 (IL-1)-dependent melanoma hepatic metastasis in vivo; increased endothelial adherence by IL-1-induced mannose receptors and growth factor production in vitro*, Natl Cancer Inst. 1996, 88, p.198-205.

27. Hacham, M. *et al*, *Complementary organ expression of IL-1 vs. IL-6 and CSF-1 activities in normal and LPS-injected mice*. Cytokine. 1996, 8, p.21-31.

28. Hacham, M. *et al, Distinct patterns of IL-1 alpha and IL-1 beta organ distribution--a possible basis for organ mechanisms of innate immunity.* Adv Exp Med Biol. 2000, 479, p.185-202.

29. Lindsay, MA. *et al, Role of miRNA-146a in the regulation of the innate immune response and cancer*. Biochem Soc Trans. 2008, 36, p.1211-5.

30. Lindsay, MA., *MicroRNAs and the immune response*, Cell, Trends Immunol. 2008, 29, p.343-51.

31. Garzon, R. Et al, *MicroRNAs in Cancer* Annu Rev Med. 2009, 60, p.167-79.

32. Taganov, K.D. *et al., NF-kappaB-dependent induction of microRNA miR-146, an inhibitor targeted to signaling proteins of innate immune responses,* Proc. Natl. Acad. Sci., 2006, 103, p. 12481–12486

33. Perry, M.M. *et al. Rapid changes in microRNA-146a expression negatively regulate the interleukin-1b induced inflammatory response in human lung alveolar epithelial cells,* J. Immunol., 2008, 180, p. 5689–5698

34. Lowell, CA, Meng F, *Lipopolysaccharide (LPS)-induced macrophage activation and signal transduction in the absence of Src-family kinases Hck, Fgr, and Lyn.,* J Exp Med. 1997, 185, p.1661-70

35. Takeshi, I. *et al, Synergic Effects of Mycoplasmal Lipopeptides and Extracellular ATP on Activation of Macrophages*, Infection and immunity, 2002, p. 3586–3591
36. Bertram, J. *et al, Establishment of a cloned line of Lewis lung carcinoma cells adapted to cell culture,* Cancer Letters, 1980, 11, p. 63-73
37. Dinarello, C. , Immunological and Inflammatory Functions of the Interleukin-1 Family, Annual Review of Immunology, 2009, 27, p. 519-550
38. Sugawara, S, *et al, Neutrophil proteinase 3-mediated induction of bioactive IL-18 secretion by human oral epithelial cells*, J Immunol, 2001, p.6568-6575
39. Gracie, JA. *et al, Interleukin-18*, J. Leukocyte Biology, 2003, 27, p. 213-224
40. Haraldsen G, *et al, Interleukin-33- cytokine of dual function or novel alarmin ?* , Trends in Immunology, Cell Review, 2009, p.227-232
41. Miyaki, S. et al, MicroRNA-140 is expressed in differentiated human articular chondrocytes and modulates interleukin-1 responses, Arthritis Rheum. 2009, 60, 9: p 2723-2730

42. Reynolds, C, & Tomayko, M, *Determination of subcutaneous tumor size in athymic (nude) mice,* Cancer Chemotherapy and Pharmacology, 1999, 24, 3, p 148-154